New Mesozoic apparent polar wander path for south China: Tectonic consequences

Zhenyu Yang, Jean Besse

JOURNAL OF GEOPHYSICAL RESEARCH, VOL. 106, NO. B5, PAGES 8493–8520, MAY 10, 2001

New Mesozoic apparent polar wander path for south China: Tectonic consequences

Zhenyu Yang
Institute of Geomechanics, Chinese Academy of Geological Science, Beijing, China

Jean Besse
Institut de Physique du Globe de Paris, Paris, France

Abstract. A new paleomagnetic study in the South Sichuan basin (South China Block) has been carried out on sediments of Early Triassic to Middle Jurassic age. Detailed stepwise thermal and alternating field demagnetizations allowed us to isolate two to three components. A low-temperature component (component A) falls close to the local present Earth field direction. A middle-temperature component (component B) is found both in limestone and red beds of Early Triassic age, in limestones of Middle Triassic age, and finally in red beds of Jurassic age. The component B directions failed the fold test but show a significant increase of the *ks/kg* ratio at 60% when a progressive stepwise unfolding is applied. The directions obtained at 60% unfolding are grouped best and yield a pole position at 76.5°N, 174.1°E, A_{95}=3.7° that is close to the Late Cretaceous pole of the South China Block (SCB) or the Early Tertiary pole of the Eurasian plate. Characteristic directions are finally obtained (component C) for Early Triassic and Early to Middle Jurassic sediments only, both with reversal and fold tests. They yield pole positions at 44.1°N and 217.2°E (A_{95}=4.9°) and 79°N and 227°E (A_{95}=4.5°), respectively. The Early Triassic result well fits other data of the same age from the SCB. The revised Late Permian to Cretaceous paleopole data provide a new Mesozoic apparent polar wander path for south China. The successive pole positions from Late Permian to Early Triassic indicate motion of the South China Block as a whole rather than local rotations linked to important strain within the block. The Early to Middle Jurassic pole is statistically indistinguishable from the compiled North China Block (NCB) poles and indicates that final suturation between the two blocks occurred by the end of the Triassic, which is coherent with the age of ultra high- pressure metamorphism in the Dabie-Sulu areas of eastern China. The Asian plate including the Mongol-Central Asian Block, NCB, and SCB, however, was probably separated from Siberia by the Mongol-Okhotsk ocean during Jurassic time.

1. Introduction

A separate paleogeographic origin of the North and South China Blocks (NCB and SCB) during the Early Paleozoic has always been strongly inferred both by the different geological nature of their basement [*Ren et al.*, 1990] and by paleomagnetic studies [*McElhinny et al.*, 1981; *Lin et al.*, 1985; *Opdyke et al.*, 1986; *Yang et al.*, 1991; *Zhao et al.*, 1990]. The final amalgamation of these two blocks occurred much later, through the presently E-W trending Qinling suture (Figure 1). This boundary is the geological consequence of successive oceanic crust subductions since the Devonian [*Mattauer et al.*, 1985] and of a later collision of still controversial age, Paleozoic for some authors [*Mattauer et al.*, 1985; *Ren et al.*, 1990] and Triassic for some others [*Hsü et al.*, 1987].

The Paleozoic age is based on the dating of ophiolite-mélange relicts in the western Qinling belt, namely, the Danfeng ophiolites of Devonian age. The occurrence of Late Triassic red molasse overlying unconformably Middle Triassic flysch formations in the Qinling belt may rather indicate a collision of Late Indosinian age between the North and South China Blocks [*Ren et al.*, 1990; *Huang and Wu*, 1992]. Indosinian orogeny is referred to as tectonic movement in east Asia from Middle Triassic to Early Jurassic.

I-type granitoid batholiths are dated around 220-200 Ma in the western part, and the occurrence of ultra high-pressure coesite eclogites dated at 235-205 Ma by Sm/Nd and U/Pb methods and 228-205 Ma by Ar/Ar dating in the Dabie-Shan area (eastern part of the Qinling) also suggest important geodynamic events related to the NCB-SCB relative motions and subsequent collision during the Late Triassic or Earliest Jurassic [*Wang et al.*, 1989; *Ames et al.*, 1996; *Gilder and Courtillot*, 1997; *Webb et al.*, 1999]. This is in agreement with paleomagnetic results, demonstrating important Mesozoic motions leading to the final collision of the NCB and SCB [*Zhao et al.*, 1990; *Yang et al.*, 1992; *Enkin et al.*, 1992b; *Gilder and Courtillot*, 1997; *Gilder et al.*, 1999].

Recent refinement in the Triassic and Jurassic segments of the NCB apparent polar wandering path (APWP) resulted from the paleomagnetic study of sediments from the Ordos basin [*Yang et al.*, 1991, 1992] and Henan-Anhui provinces [*Gilder and Courtillot*, 1997]. The precision of this path can be considered

Paper number 2000JB900338.
0148-0227/01/2000JB900338$09.00

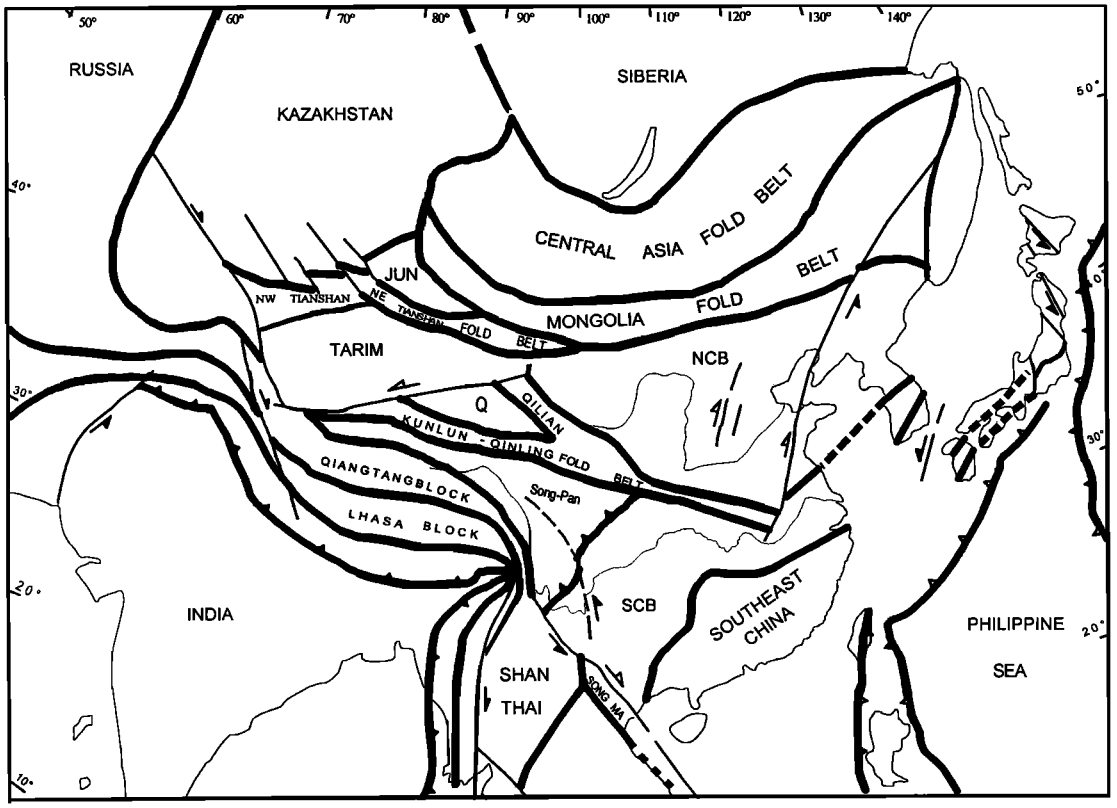

Figure 1. Tectonic sketch map of eastern Asia. The main blocks (Siberia, Central Asian Fold belt, North China Block, South China Block, southeastern China Block, Indochina, India, Kazakhstan, and Tarim blocks) are recognized (modified from *Yang et al.*, [1992]). Arrows correspond to the sense of strike-slip motion along major faults (closed for the period before 20 Ma, open between 20 and 0 Ma) [*Tapponnier et al.*, 1982]. Heavy lines are for sutures or main boundary faults, and thin lines are for strike-slip faults.

now as satisfactory. On the other hand, *Yang and Besse* [1993] emphasized paleomagnetic uncertainties in large parts of the Mesozoic SCB APWP. The Early Triassic pole is well determined by numerous consistent studies extensively distributed all over the Yangtze craton (SCB) [*e.g.*, *Opdyke et al.*, 1986; *Heller et al.*, 1988; *Steiner et al.*, 1989; *Enkin et al.*, 1992a; *Heller et al.*, 1995]. However, the three Mesozoic apparent polar wander paths (APWP) compiled for south China [*Lin et al.*, 1985; *Enkin et al.*, 1992b; *Wang et al.*, 1993] are at strong variance during the Middle Triassic to Middle Jurassic age range. As a consequence, the chronology of relative motions and collision between the SCB and NCB is also a matter of paleomagnetic debate. As part of a cooperation project between the Chinese Academy of Geological Sciences and the Institut National des Sciences de l'Univers, we have sampled the Triassic and Early to Middle Jurassic sequences from the Xuyong areas in the South Sichuan basin.

2. Geological Setting and Sampling

The Triassic system of the South China Block, with rather continuous well-developed sedimentary sequences, has been extensively studied [*Yang et al.*, 1986]. Outcrop exposures are excellent, particularly in the Sichuan basin. The area of our study (Figures 1 and 2) is located in the south of the basin, and includes the Early Triassic Feixianguan and Jialinjiang Formations, which overly conformably Late Permian limestones.

The Feixianguan Formation consists of shallow water marine deposits. Purplish-red siltstones and sandy shales are intercalated by oolitic limestone. Marls are found in the upper part of the section, while oolitic or argillaceous limestones and marls are found in the lower part. From bottom to top the Jialinjiang Formation comprises laminated calciferous siltstones and limestones, gray to black thick limestones, oolitic limestone, marls, brecciated limestones, and finally limestones and dolomitic limestones in the uppermost part. Paleontological studies have show evidence of five conodont zones, indicating that the Feixianguan Formation encompasses the Griesbachian and Nammalian stages and the overlying Jialinjiang Formation encompasses the Spathian stage (Early Triassic) [*Yang et al.*, 1986].

The overlying Middle Triassic Leikoupo Formation is composed of dolomitic limestones intercalated with marl and mudstone. A layer of volcanic ash some 0.5 m thick, which marks the Early-Middle Triassic boundary, is found everywhere in the Sichuan basin. This layer is called "zone of the mung bean stone" [*Bureau of Geology and Mineral Resources of Sichuan Province (BGMRS)*, 1991].

The Sichuan basin has been affected by tectonic activity probably as early as during the Late Triassic, as shown by a sedimentation change from marine to fluvio-deltaic facies, however conformably overlying Middle Triassic strata. The Late Triassic Xujiahe Formation is made of green to gray arkose,

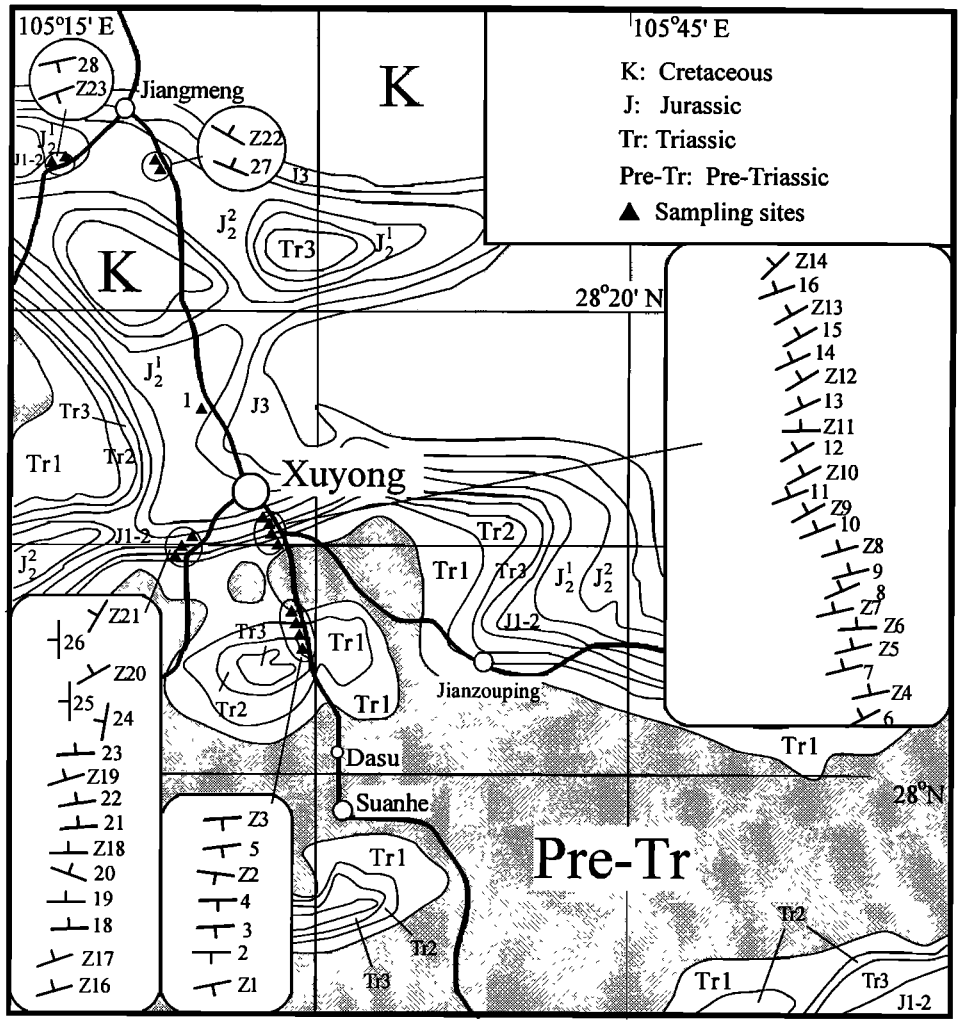

Figure 2. Simplified geologic map of the sampling area at Xuyong, Southern Sichuan basin (modified from *BGMRS,* [1991]), with sampling sites indicated as black triangles. Strike direction for each sampling site is shown in insets.

sandstone, black shales, and siltstones, which are sometimes interbedded with coal strings.

The Jurassic sediments of this region consist almost entirely of red beds comformably deposited on Triassic series. The Early Jurassic Ziliujing Formation is made up of red to gray mudstones, sandy mudstone interbedded with arkose, and siltstone, which yields fossils such as *Pseudocardinia elongatiformis, P.; gansuensis, P. cf. Sibirensis, and P. hupehensis Modiolus cf. Yunlongensis* [*BGMRS,* 1991].

The overlying Middle Jurassic comprises the Shaximiao and Suining Formations. Clastic rocks characterize the Shaximiao Formation. Purplish-red sandstone, siltstone, mudstone, and marl containing rich estherids (*Euestheria gr.*) and ostracods are found. The Suining Formation consists mostly of brick red to purplish-red mudstones and sandstones.

The Jurassic ends with the Late Jurassic Penglaizhen Formation, which is composed of purplish-red coarse sandstone interbedded with arkose and a few mudstones.

The unconformity of the Eocene over older series [*BGMRS,* 1991; *Lee,* 1950] indicates a pre-Eocene phase of deformation, generally related to the latest phase of the Yanshanian orogeny (Late Cretaceous to Early Tertiary). However, this unconformity is not observed in our region, and a folding age related to the India/Asia collision cannot be excluded completely. The local direction of folding for the Triassic, Jurassic, and the Late Cretaceous Jiaquan Formation trends E-W, while the trend of the strong folds in the eastern Sichuan basin is rather SW-NE.

We have sampled a total of 51 paleomagnetic sites in the Xuyong area (Figure 2), which includes 19 Early Triassic sites, 9 Middle Triassic sites, and 6 Late Triassic sites. Seventeen Early and Middle Jurassic sites representing the Ziliujing Formation to Suining Formation were also collected in both flanks of a syncline. Samples were obtained using a portable drill and oriented with a magnetic compass. In the laboratory, 2.2 cm long specimens were sliced for further measurements.

3. Paleomagnetic Results

Natural remanent magnetization (NRM) measurements were made using a three-axis CTF cryogenic magnetometer in a magnetically shielded room at the paleomagnetic laboratory of the Institut de Physique du Globe (IPG) in Paris. Some red sandstones

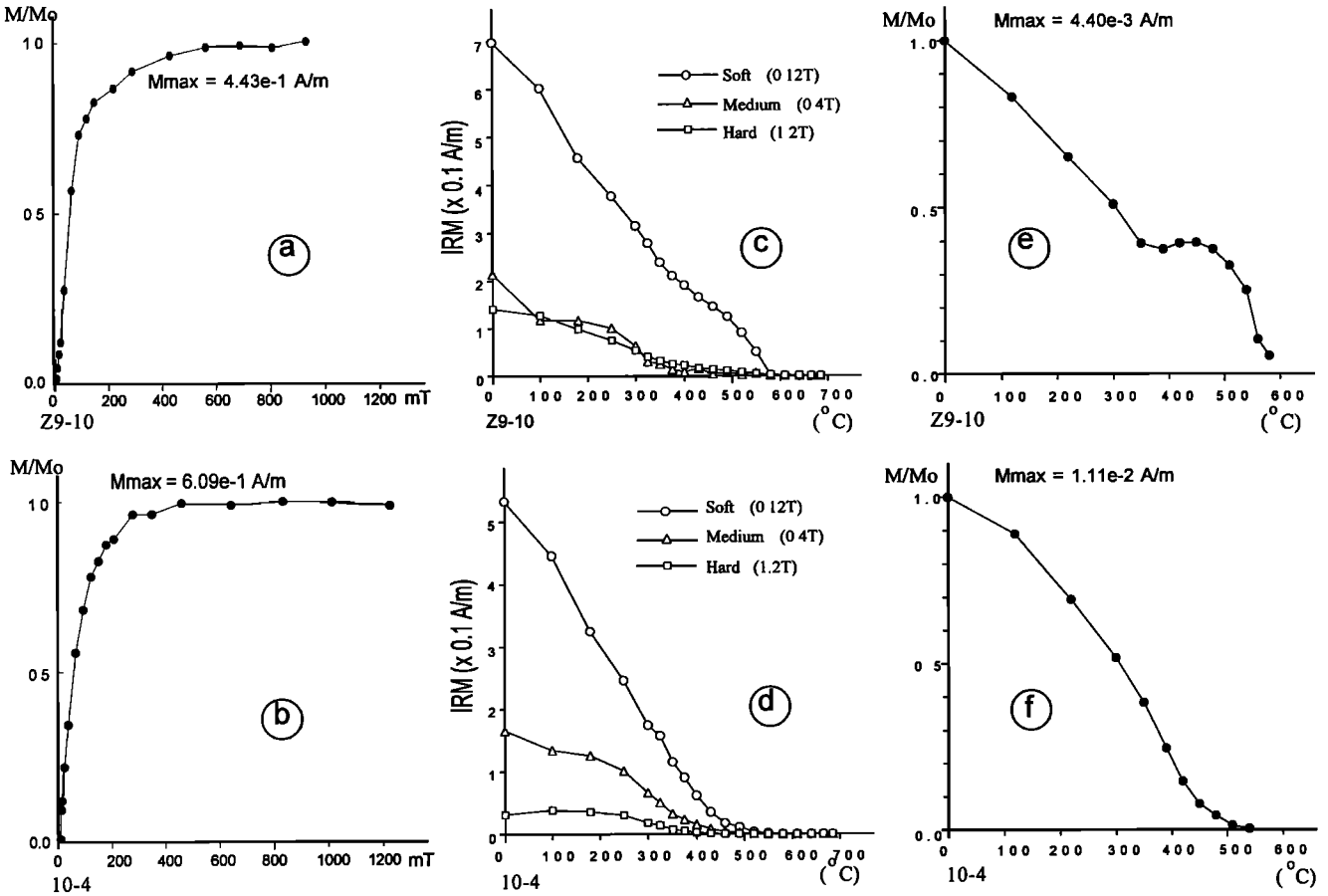

Figure 3. (a, b) Normalized isothermal remanent magnetization (IRM) acquisition curves; (c, d) three-component IRM thermal demagnetization showing unblocking temperatures around 450 and 580 °C, respectively; (e, f) natural remanent magnetization (NRM) whose thermal demagnetization indicates a similar behavior as that of the IRM. Open circles indicate soft component, 0.12T field; triangles indicate medium component, 0.4T field, and squares indicate hard component, 1.2T field.

were measured using a Schonstedt DSM-2 spinner magnetometer in the paleomagnetic laboratory at the Chengdu Institute of Geology (China). Stepwise alternating field and thermal demagnetization (up to more than 10 steps) was used to separate the magnetic components for all specimens, using a Schonstedt GSD-1 demagnetizer and a laboratory-built oven in Paris and a Schonstedt thermal demagnetizer in the Chengdu laboratory. The bulk magnetic susceptibility of the specimens was measured at each demagnetization step in Paris in order to monitor magnetic mineral alteration during progressive heating. Principal component analysis was used to separate and calculate the different magnetic components, and site-mean directions were calculated using *Fisher*'s [1953] method or *McFadden and McElhinny* [1988] statistics.

3.1. Early Triassic Results

Two kinds of rocks (red siltstones and limestones) have been sampled in the Early Triassic Feixianguan Formation. In the Jialinjiang Formation we sampled only limestones. In total, 19 sites were sampled (Figure 2). The red bed samples show a higher intensity of the natural remanent magnetization (NRM) than the limestones (50 and 10 mA/m, respectively).

3.1.1. Limestone specimens. Isothermal remanent magnetization (IRM) acquisition in limestone specimens shows that saturation is achieved after applying a field of ~0.3 T (Figures 3a and 3b). In order to better identify the magnetic fractions we have also used the thermal demagnetization of isothermal remanent magnetizations (IRM) successively applied in different fields (1.26, 0.4, 0.12 T) and along three orthogonal axes of a sample as described by *Lowrie* [1990]. Thermal demagnetization of the IRM shows the predominance of low coercivity minerals with two different unblocking temperatures spectra at around 450°C and 580°C, respectively (Figures 3c and 3d). A similar characteristic is also evidenced by thermal demagnetization of the natural remanent magnetization (NRM) (Figures 3e and 3f). However, the highest unblocking temperature is well marked in the example shown in Figure 3f, while it appears to be more attenuated in the example of Figure 3e. The low coercivity and the unblocking temperatures lower than 580°C suggest a different grain size of magnetite family as the carrier of remanence.

Two or three NRM components are found in the limestones. A first component (component A) is isolated in most samples below 200°C and corresponds to the present Earth field (PEF) before bedding correction (Figure 4). A second component is determined by a well-defined linear segment including at least three

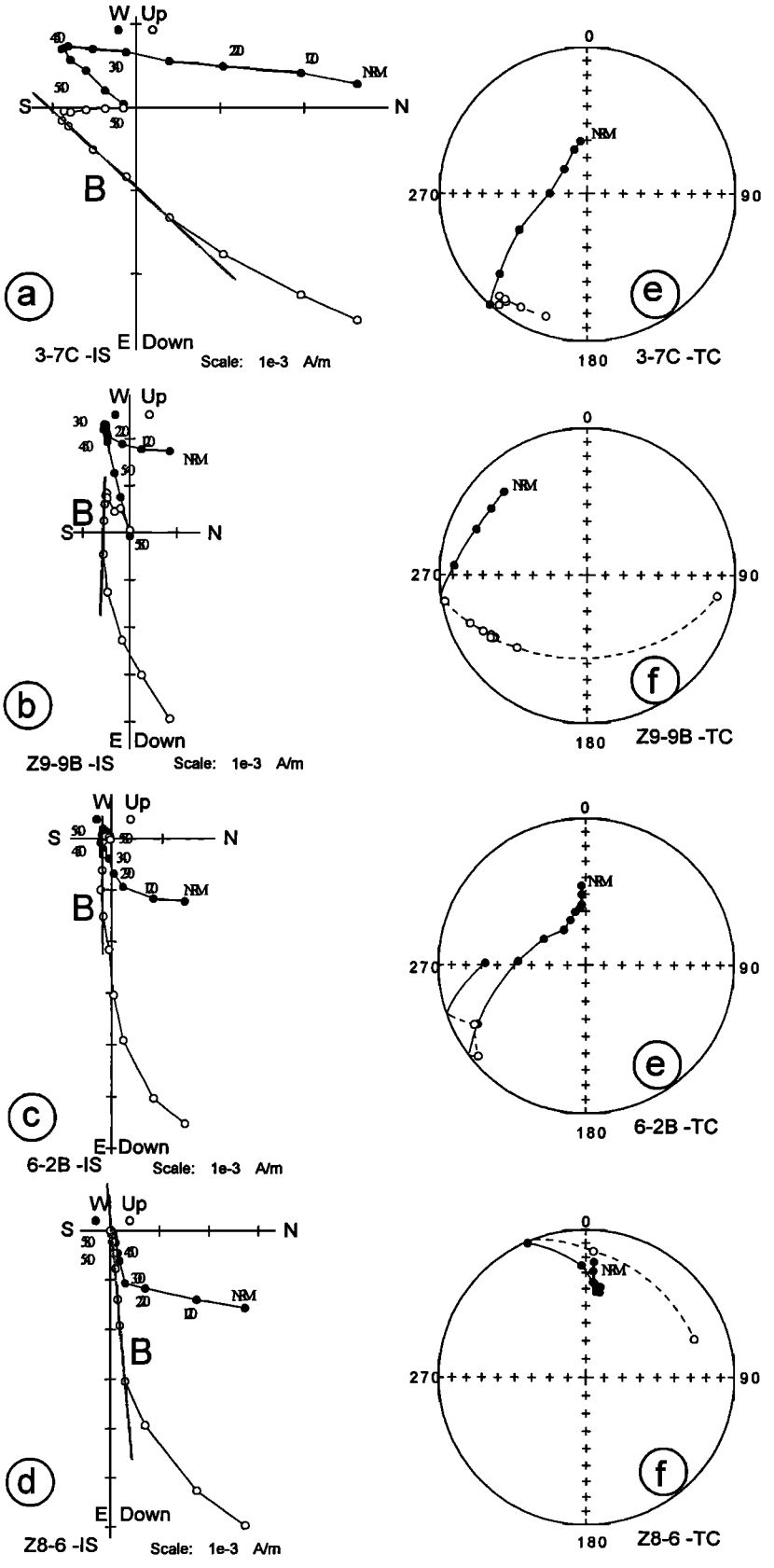

Figure 4. (a to d) Orthogonal vector projection of thermal demagnetization in situ and stereoplot (e to h) of magnetic direction changes after tilt correction of Early Triassic samples from the Xuyong area. Solid (open) symbols refer to the projection on the horizontal (vertical) plane. Stereoplot with solid (open) symbols in the lower (upper) hemisphere.

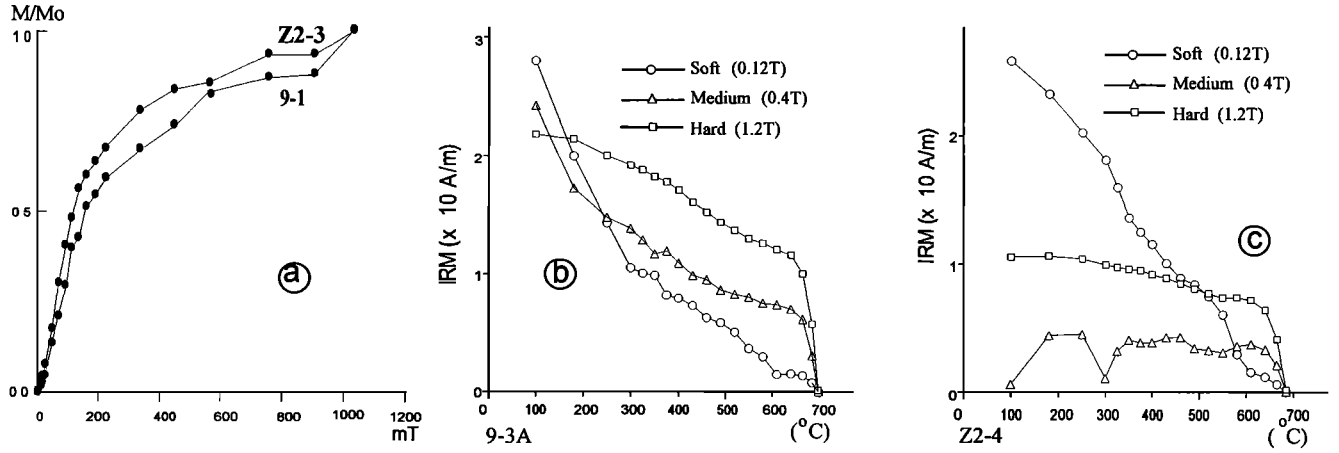

Figure 5. (a) Normalized isothermal remanent magnetization (IRM) acquisition curves; (b, c) three-component IRM thermal demagnetization showing unblocking temperatures around 580 and 680°C, respectively, for the Early Triassic red siltstone samples. Symbols are same as in Figure 3.

demagnetization steps on the orthogonal vector diagrams. This component (component B) occurs between 220° and 400-450°C in most samples. The highest unblocking temperature component (component C) is determined between 400-450°C and 510-580°C. With the exception of one site (Figure 4, Z8-6), its direction is of reversed polarity. Component C may be overlapped completely by component B. Three types of behavior are shown in Figure 4. Figures 4a and 4b show a linear decay of component C to the origin from 450°C to nearly 580°C, yielding an easy determination of its direction. Figure 4c shows a stronger overlap of components B and C, but a great circle can be used for the determination of directions (Figure 4c) [*McFadden and McElhinny,* 1988]. Finally, the sample shown in Figure 4d displays component B only. Components A and B are found only in three limestone sites (10, 11, and Z8). The unblocking temperatures from 450°C to 580°C may signify a different grain size family of magnetite.

3.1.2. Sandstone specimens. IRM acquisition on two typical red sandstone specimens shows that saturation is not achieved after applying a field of 1.2T (Figure 5a). The thermal demagnetization of IRM clearly shows the presence of high coercivity minerals (Figures 5b and 5c) with unblocking temperatures of 680°C, indicating the presence of hematite. The presence of low-coercivity minerals showing clearly a strong decay of intensity before 580°C (Figure 5c) along with the saturation of 60% at 0.2 T (Figure 5a) also suggests the possible presence of the titanomagnetite minerals for some sites. Three NRM components are recognized in the sandstone samples. A component A, for which in situ directions are close to the PEF, is separated below 380°C (Figures 6a-6c). A different component B (with the same direction and same normal polarity as the component B at the limestone sites) is determined between 380°C and 600-620°C. A component C of either reversed or normal polarity is moreover revealed up to 690°C from the red bed samples. This confirms the presence of high-coercivity minerals (hematite) evidenced by the IRM acquisitions and its thermal demagnetization (Figures 5a-5c). Only a few component C decaying linearly to the origin could be determined (Figures 6a and 6b). A strong susceptibility increase at 600-650°C witnesses an important mineralogical transformation which prevents the determination of the final directions (Figure 7a). Indeed, directions after 650°C become erratic, but well-defined great circle paths at temperatures lower than 650°C are shown on the stereographic plot (Figures 6c and 7b). The site-mean direction is then computed using the intersection of sector-constrained great circles combined with directly observed directions (Figure 7b) by using the statistical method developed by *McFadden and McElhinny* [1988]. Both normal and reversed polarities are found. Most sites are of reversed polarity, with the exception of site 5 of mixed polarity and site 8 of normal polarity.

Each component (A, B, or C) has similar directions in the limestones and in the sandstones. A mean direction of D =5.6°, I= 45.4° (N =18 and α_{95} =4.0°) is found for component A before tilt correction, indistinguishable from the PEF (D =0° and I =47°). The decrease of the precision parameter (k) from 77 to 8 after tilt correction shows that this component has been acquired after folding.

The tilt correction improves the grouping of site-mean directions for the component B (Figures 8a and 8b). However, progressive stepwise unfolding shows that the ratio of precision parameters before any correction and after progressive correction (*ks/kg*) passes through a maximum at a value of 60% (Figure 8c). This characteristic may indicate that component B is probably a remagnetization acquired during the folding.

Finally, the tilt correction greatly improves the clustering of site-mean directions for component C (Figures 9a and 9b). The ratio of precision parameters is maximum at a 100% unfolding (Figure 9c). The average site-mean direction is D= 233.7°, I=-17.8°, α_{95} =12.7° before, and D = 222.1°, I = -10.2° and α_{95}=6.8° (*ks/kg* =33.1/10.1) after tilt correction (Table 1). The fold test is positive at the 99% probability level according to the fold tests of *McElhinny* [1964] and *McFadden* [1990]. Our Early Triassic pole study comes from two different lithologies (sandstones and limestones) with a magnetization carried both by hematite and magnetite and passes successfully the fold test and possesses both normal and reversed directions. It most likely represents the original direction. Directions are summarized in Table 1.

3.2. Middle Triassic Limestone

The acquisition and thermal demagnetization of the IRM on two samples (Figure 10a) is very similar to that of the Early Triassic limestones (Figures 3d and 3e): saturation is reached in a field of 200-300 mT. Low-coercivity minerals with unblocking

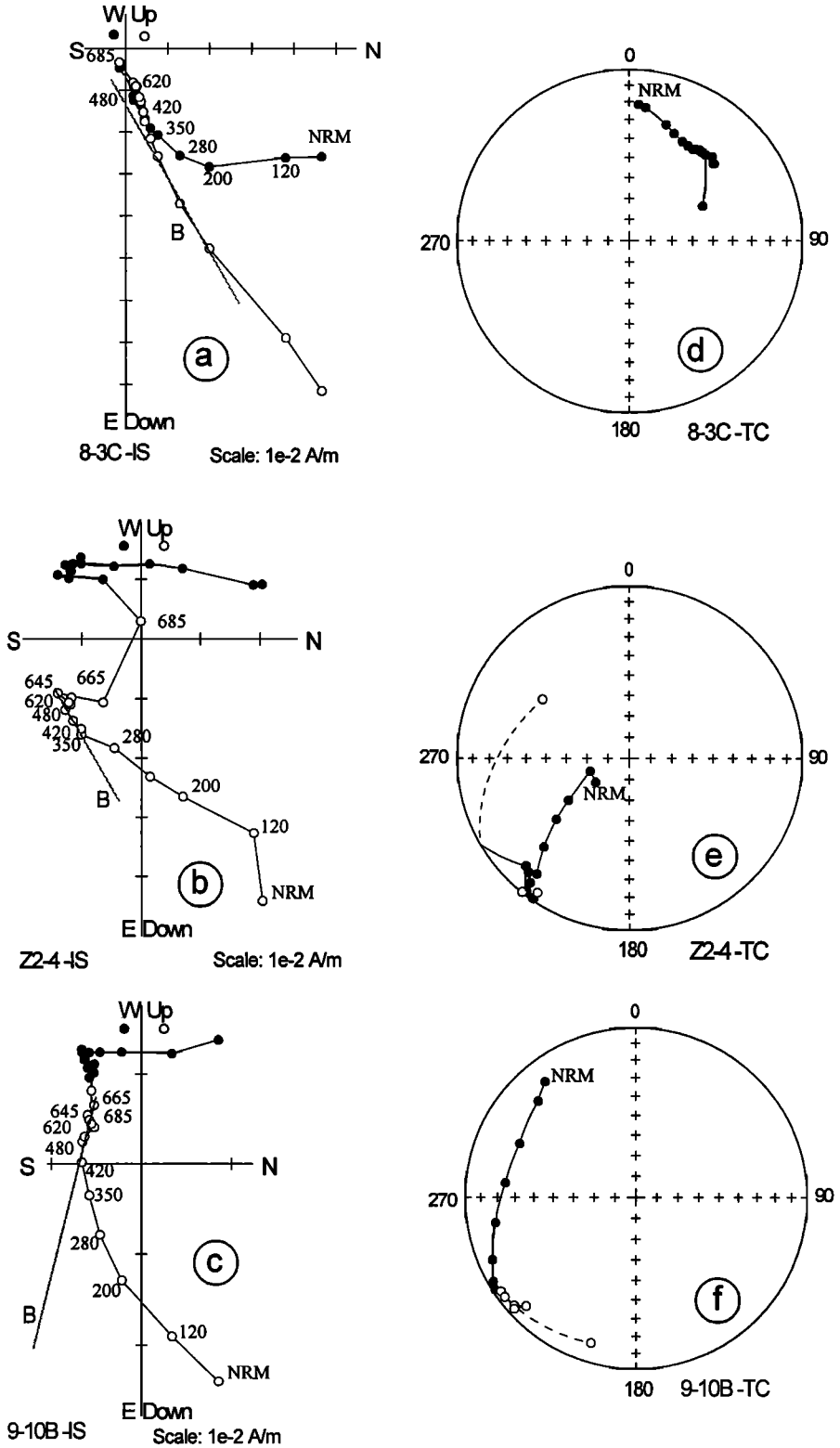

Figure 6. (a to c) Orthogonal vector projection of NRM thermal demagnetization in situ, and (d to f) stereoplot of directional changes after tilt correction of Early Triassic siltstone samples from the Xuyong area. Symbols are same as in Figure 4.

temperatures predominantly between 450°C and 550°C suggest the presence of a different grain size of magnetite minerals (Figure 10b). Two NRM components (A and B) are isolated (Figures 11a-11c). The direction of component A determined between 120°C and 220°C is close to the PEF direction. The component A directions are dispersed into two groups after bedding correction, indicating a post-folding overprint. Component B is evaluated from 300°C to 540°C. The site-mean directions of the magnetic component B converge into one group after bedding correction, as shown on Figures 12a and 12b. However, the directions of this

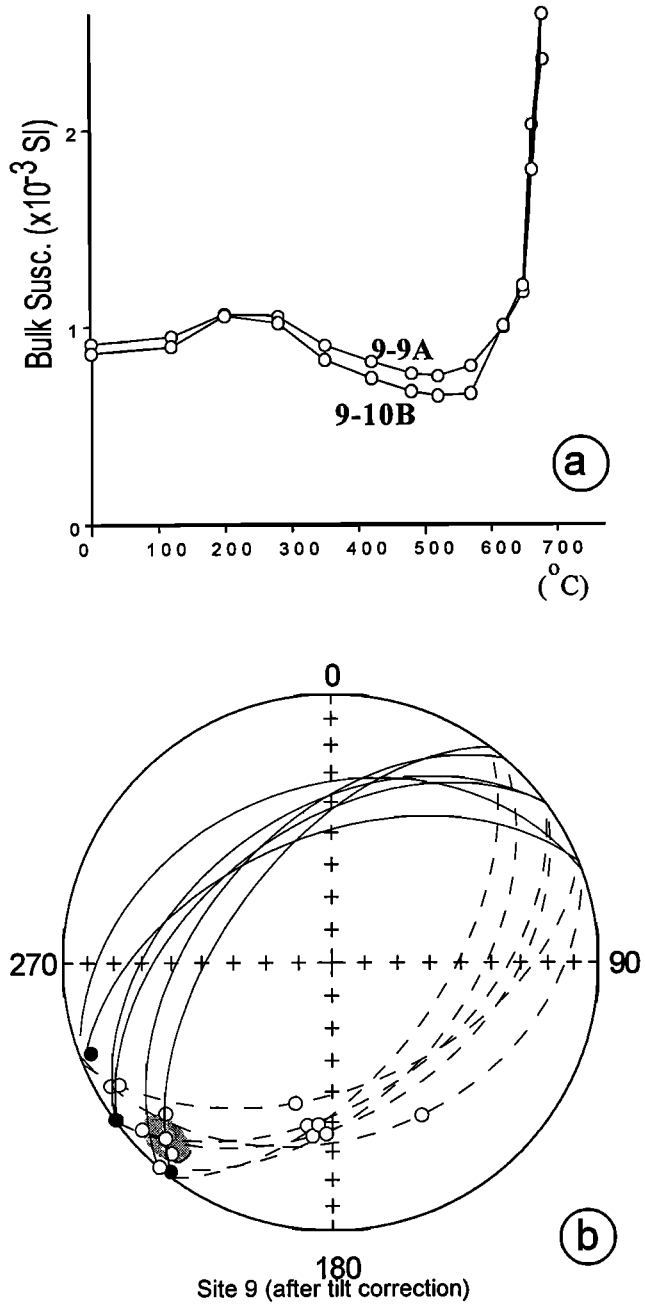

Figure 7. (a) Bulk susceptibility change during heating and (b) the mean direction calculated from the intersection of the great circles with limiting sector constraints for the Early Triassic siltstone specimens of site 9. Symbols are same as in Figure 4.

component B and the Early Triassic component B appear to be similar (D=13°, I=52.7°, α_{95}=3.9° and D=23.9°, I=62.2°, α_{95}=6.0°, respectively). The ratio of the precision parameters before and after correction of the bedding attitude (*ks/kg*) is maximum at an unfolding value of ~70% (Figure 12c). A secondary origin of the remanence is suggested. The directions are summarized in Table 2.

3.3. Late Triassic Results

Typical IRM acquisition and IRM thermal demagnetization of two samples of sandstones show that saturation is reached in a field of 200-300 mT, while low-coercivity minerals with unblocking temperatures at 580°C again suggest the presence of magnetite. Specimens from six sites have been measured using thermal demagnetization up to 580°C. Owing to unstable directional behavior during the demagnetization process, only a PEF component could be separated. A composite demagnetization was then attempted, heating first up to 225°C and then demagnetizing with alternating fields up to 50 mT (Figure 13). This method also led to an erratic behavior of the directions during AF treatment. We have thus discarded all these sites.

3.4. Early-Middle Jurassic Results

Seventeen sites of Jurassic red beds and gray sandstones were thermally demagnetized. The IRM acquisition shows that saturation is still not reached at a field of 0.5 T (Figure 14a). The thermal demagnetization of IRM clearly shows the presence of high-coercivity/high unblocking temperature (690°C) hematite minerals (Figure 14b).

The NRM thermal demagnetization behavior, however, can be separated into three categories. In the first category, three NRM components, as for most samples of Early Triassic age, can be isolated, which are a low-temperature component (A) close to the PEF from NRM to 180°C, a middle temperature component (B) from 180°C to around 500°C, and a final third component (C) from 500°C to 680°C. Examples of thermal demagnetization are given in Figure 15 for a normal and a reversed sample. Indeed, samples of normal and reversed polarities are found in 7 out of 17 sites.

In the second category, NRM directions become erratic at around 550 to 600°C, probably due to magnetic mineral changes (Figures 16a and 16b). The final component direction is estimated using remagnetization great circle (Figures 16c and 16d) intersections [*McFadden and McElhinny,* 1988]. An example of the mean direction computed using the great circle intersection method is shown in Figure 16e for site Z21. Several sites were rejected since the dispersion during demagnetization did not allowed us to fit great circles.

In the third category, a single component of direction close to the PEF direction (not shown) could be defined during stepwise thermal demagnetizations. The site-mean directions of a lower-temperature component A are close to the PEF before bedding correction and fail the fold test. The site-mean directions of a middle-temperature component B are not significantly better clustered after than before bedding correction. As for the Early and Middle Triassic sediments, the ratio *ks/kg* passes a maximum at around 60% unfolding (Figures 17a-17c).

Finally, five sites of normal and five sites of reversed component C polarity with antipodal directions pass the reversal test of *McFadden and McElhinny* [1990] at the 95% probability level (B class). A positive fold test (unfolding at 100%) is also passed successfully at the 99% level (Table 3 and Figures 18a-18c). This component may likely represent the original magnetization.

4. Discussion

4.1. Remagnetization

Component B was found in all sites using progressive stepwise unfolding. A maximum k ratio is found at around 60% unfolding for both Early Triassic and Early-Middle Jurassic sediments. The direction issued appears coherent from one site to another with D =13.0° and I =52.7° (α_{95} =3.9°) in the Early Triassic sediments

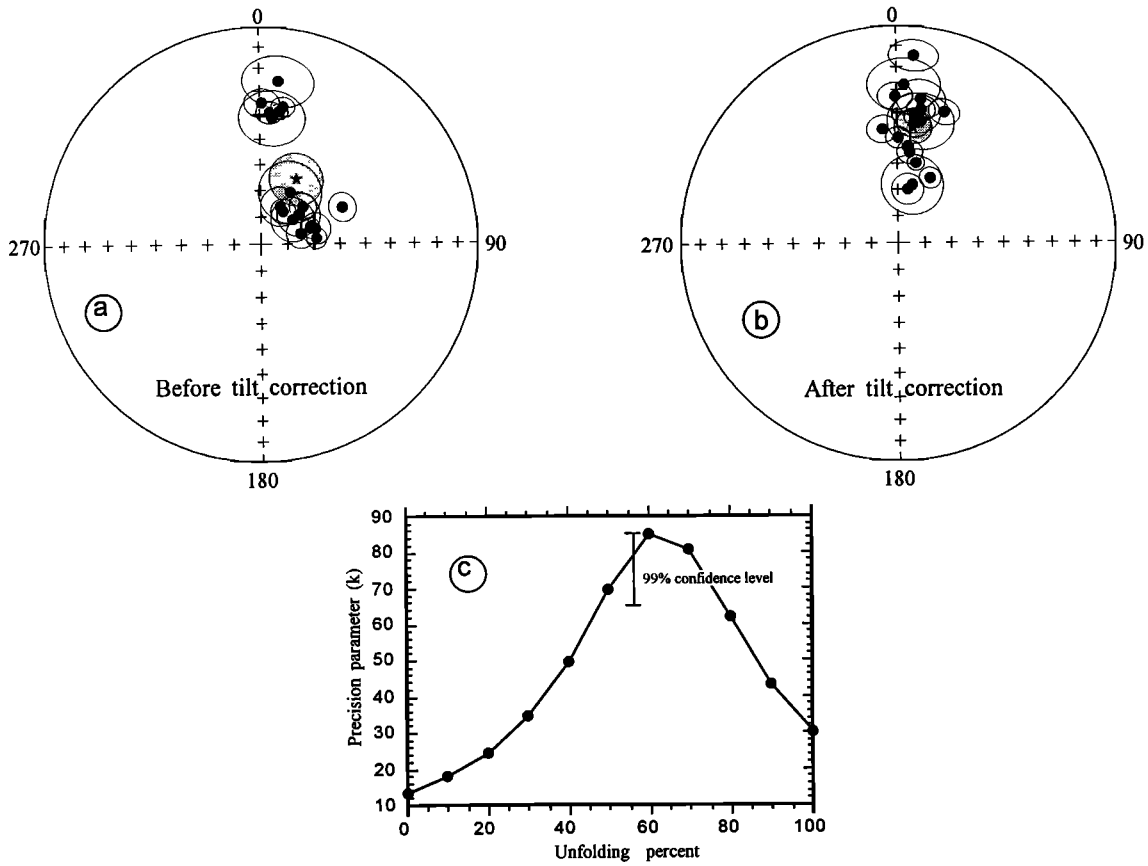

Figure 8. (a, b) Equal-area projection of the component B site-mean directions for the Early Triassic before and after tilt correction. Stereoplot with solid symbols in the lower hemisphere. (c) Maximum of the precision parameter at 60% unfolding.

and D =13.9° and I =51.9° (α_{95}=4.4°) in the Early-Middle Jurassic sediments. This direction has also been found by *Enkin* [1990] and *Enkin et al.* [1992a] in the Permian and Triassic sediments from the south-eastern part of the Sichuan basin. It was given (at 50% unfolding) as D =17.8°, I =52.1° (α_{95} =7°, N=7 sites) and appears to be statistically indistinguishable from our directions. *Enkin et al.* [1992a] questioned whether this direction would be an unseparable combination of a prefolding Mesozoic overprint and a post folding present field overprint or the result of a synfolding remanence. Its consistent presence in other remote sites suggests that it constitutes a general synfolding remagnetization of this region. The three results [*Enkin et al.*, 1992a; this study] provide a synfolding pole at 76.5°N, 174.1°E (A_{95}=3.7°), situated in the confidence ellipse of the Late Cretaceous pole from the NCB and SCB (Figure 19), which may correspond to the late phases of the Yanshanian orogeny [*Ren et al.*, 1990].

The direction is different from the one proposed by *Wang et al.* [1993]. They characterized a "folding-associated" remagnetization leading to a Triassic/Jurassic loop. Their interpretation was based on remagnetizations of Middle Triassic rocks from South Guizhou province (500 km away from our sampling area). Such folding-associated pole determination comes up against two major problems. The first one concerns the determination of the paleohorizontal during the acquisition of the remagnetization. The second is the precise estimation of the folding age. They assumed that the folding time was close to the Triassic/Jurassic boundary age. However, field evidence for such a phase is lacking. Indeed, the Triassic and Early and Middle Jurassic series are generally folded together in the Zhenfang area and overlain by Late Cretaceous sediments, in agreement with the age of the late Yanshanian orogeny in North Guizhou and South Sichuan basin. The so called folding-associated remagnetization was probably acquired between Middle Jurassic and Late Cretaceous. On the other hand, *Huang and Opdyke* [1996b, 1997] declared that no evidence of a similar remagnetization was found in their samples, but their remagnetized paleopole related to Jurassic and Cretaceous folding is close to our synfolding pole (Figure 19).

4.2. Mesozoic Apparent Polar Wander Path for the South China Block

4.2.1. Permo-Triassic boundary and Early Triassic. The Permo-Triassic boundary sections of south China are stratigraphically complete and considered as candidates for International Stratotype sections. They have been intensively investigated for magnetostratigraphic studies [*Steiner et al.*, 1989; *Heller et al.*, 1988, 1995; *Dobson et al.*, 1993]. The large number of available studies thus allows division of the pole list into two time periods, the Permo-Triassic boundary (Figure 20a) and the Early Triassic (Figure 20b). In Figures 20a and 20b the coherence between the selected poles appears to be excellent: the P/T

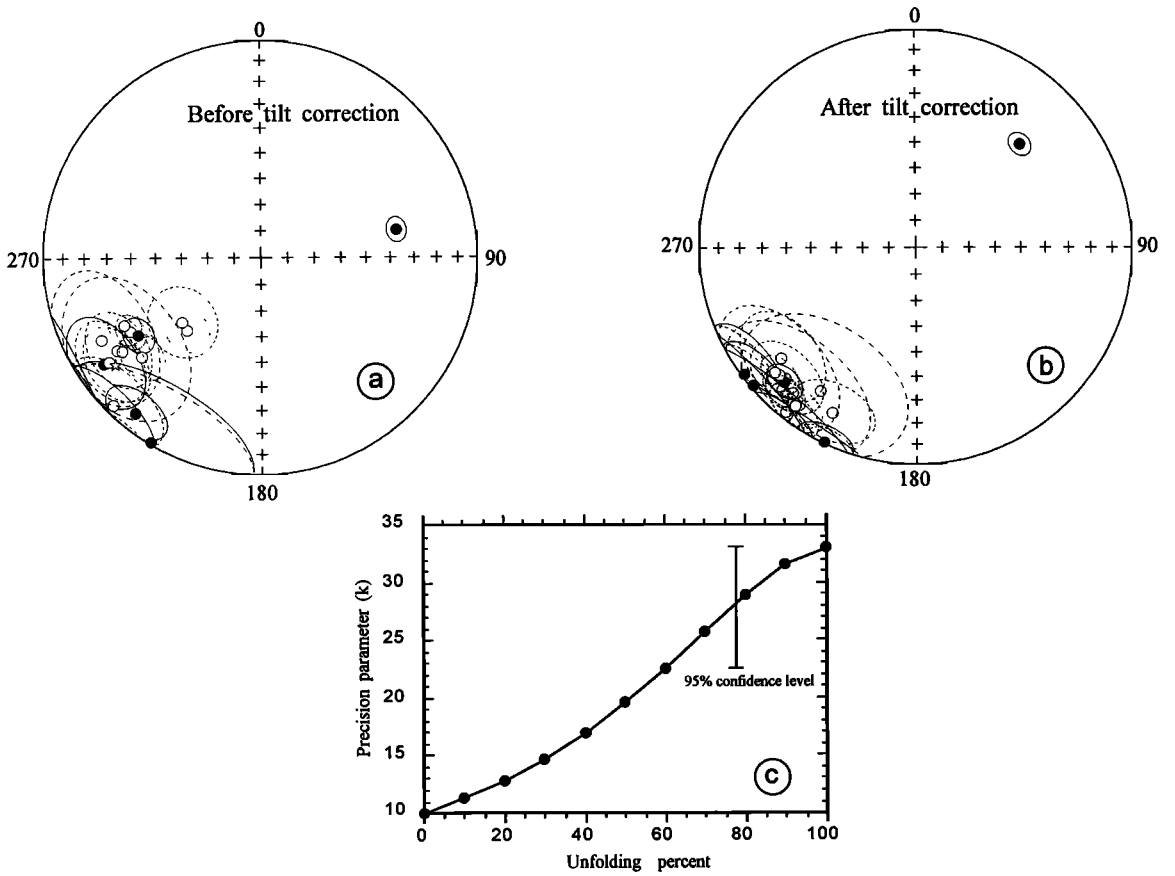

Figure 9. (a, b) Equal-area projection of the component C site-mean directions for the Early Triassic sediments before and after tectonic tilt correction, and (c) the change of the precision parameter (k) during unfolding up to 100%.

individual means are in the intersections of other confidence ellipses and a mean pole position at λ=48.8°N, ϕ=227.7°E, A_{95}=3.1° is resulting. Paleomagnetic sites are coming from extreme west (Sichuan) and extreme east (Zhejiang) of the SCB (Figure 20a), underscoring no relative important rotations between these distanct sites.

The paleopoles of Early Triassic age also cluster well. We have additionally used one of the Permo-Triassic boundary poles of *Steiner et al.* [1989] which mostly comprises Early Triassic samples. With the exception of one pole [*Zhu et al.*, 1988], which appears to be a clear outlier (Figure 20b), almost all poles fall in a very narrow area: the resulting Early Triassic mean pole

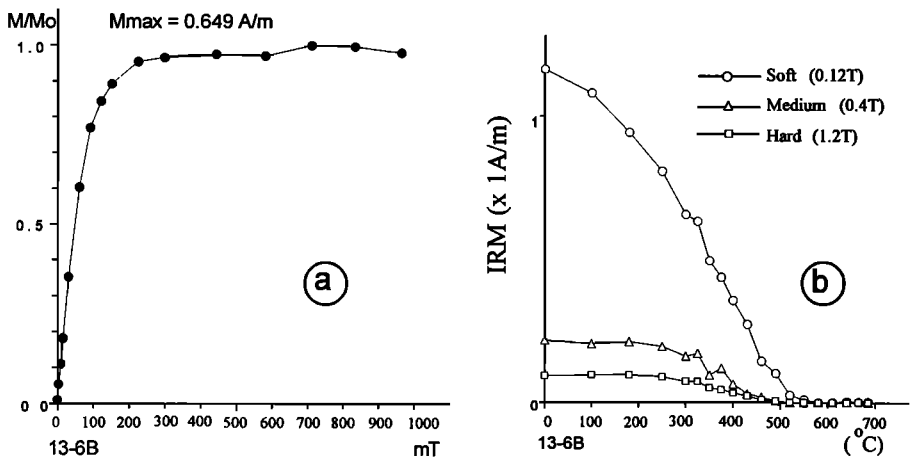

Figure 10. (a) Normalized isothermal remanent magnetization (IRM) acquisition curves; and (b) three-component IRM thermal demagnetization showing unblocking temperatures around 530°C for the Middle Triassic limestone samples.

Table 1. Lower Triassic Site-Mean Directions and Corresponding Poles From the Xuyong Area (28°N/105.5°E)[a]

Site	*n*	In Situ		Tilt Corrected				Pole	
		D	*I*	*D*	*I*	*k*	α_{95}	λ(°N)	Φ(°E)
				Middle-Temperature Component B (200°- 400°C)					
10	6	74.8	68.6	8.0	43.5	136.3	5.8		
11	8	84.4	68.9	0.5	49.7	163.7	4.3		
2	6	8.5	38.2	12.9	58.9	474.1	3.1		
3	4	4.3	39.0	7.7	55.2	399.1	4.6		
4	4	5.6	41.0	14.1	67.4	66.1	11.4		
5	9	9.8	35.9	26.6	62.7	167.4	4.0		
6	6	70.9	70.0	6.3	53.1	960.0	2.2		
7	2	30.0	67.6	2.6	27.7	447.9	11.8		
8	5	66.2	56.0	19.8	36.1	205.8	5.3		
9	10	34.8	75.2	359.3	32.7	71.0	5.8		
Z1	5	6.7	25.3	11.0	42.2	45.4	11.5		
Z3	8	0.9	35.0	10.4	69.5	90.4	5.9		
Z4	13	52.5	72.0	8.4	39.3	26.7	8.2		
Z5	4	27.7	74.2	5.3	14.2	153.1	7 4		
Z6	5	52.9	75.0	9.4	33.1	87.4	8.2		
Z7	12	48.9	68.9	10.2	37.5	82.0	4.8		
Z8	6	72.4	70.5	8.2	41.0	313.1	3.8		
Z9	7	75.7	74.5	352.7	45.9	123.5	5.5		
Mean	18	29.2	62.1	-	-	12.8	10.0		
Mean	18	-	-	7.8	45.2	28.5	6.6		
Mean[b]	18			13.0	52.7	80.0	3.9	77.6	167.0
								dp=3.7°,	*dm*=5.4°
				Higher-Temperature Component C					
2	6	236.0	13.7	233.7	1.6	25.0	15.2	31.1	215.3
3	4	219.0	8.6	218.5	-3.4	84.2	10.1	44.8	224.8
4	3	211.0	1.0	213.8	-21.3	553.2	28.4	54.1	216.9
5	9	225.1	-4.2	230.7	-20.4	12.3	16.0	39.5	205.3
6	4	237.2	-22.3	225.0	-15.5	94.0	13.0	43.1	212.0
7	4	235.5	-16.2	229.9	1.7	86.1	13.6	34.2	217.9
8	7	78.4	36.3	45.5	32.8	257.7	4.2	47.1	199.1
9	9	240.5	-31.5	223.4	-10.6	65.2	6.8	43.0	216.1
11	5	236.0	-23.9	220.4	-12.8	15.3	25.0	46.1	217.1
Z3	8	237.8	33.5	224.5	14.0	88.3	6.3	34.5	227.9
Z4	12	243.7	-30.4	227.1	-14.6	46.9	6.8	41.0	211.1
Z5	4	225.5	-50.4	205.5	0.7	470.0	8.2	52.6	240.4
Z6	5	230.7	-51.1	207.0	-15.3	72.7	13.2	57.5	228.7
Z7	10	230.3	-29.3	217.5	-8.7	38.6	8.6	47.0	222.1
Z9	4	242.7	-18.5	228.6	-13.9	18.1	22.2	39.6	210.5
Mean	15	233.7	-17.8	-	-	10.1	12.7		
Mean	15	-	-	222.1	-10.2	33.1	6.8		
Mean	15						4.9	44.1	217.2

[a] *n*, number of specimens (or sites); *D*/*I*, declination/inclination before or after tilt corrections; *k*, precision parameter after tilt correction; α_{95}, half angle of cone of 95% confidence about the mean direction in stratigraphic coordinates; λ/Φ, latitude/longitude of virtual geomagnetic pole; *dp*/*dm*, axes of ellipse of uncertainty of the pole; [b]mean at 60% unfolding level. Fold test for the higher temperature component C, (1) *McElhinny*'s[1964] method, *ks*/*kg*=3.3 > *F*(28, 28)=2.47 at 99% confidence level, and (2) *McFadden*'s[1990] fold test, ξ_1=10.44 in geographic coordinate and ξ_2=1.791 in stratigraphic coordinate, critical value of the test statistic ξ =6.3 at 99% confidence level indicative of positive fold test.

(λ=42.5°N, ϕ=213.9°E, A_{95}=2.7°) is therefore particularly well defined. Our pole from the Xuyong area (λ=44.1°N, ϕ=217.2°E, A_{95}=4.9°) is identical to the mean pole of all other sites. Again, the Early Triassic poles come from widespread sampling on the SCB. Poles from the Guizhou, Sichuan, and the Emei-Shan regions (Sichuan) are included in this list and cluster well (Figure 20b). The data for the P/T boundary and the Early Triassic do not strike along small circles centered on the sites as suggested by *Enkin et al.* [1992b]. From east to west, no appreciable relative rotations between sites can be found. This appears to be true also for the Triassic of the Emei-Shan region. These poles are statistically distinct from each other and also statistically distinct from the Late Permian pole of *Enkin et al.* [1992b] (Figure 21). Hence the small circle dispersion corresponds to a polar motion along a track rather than to local rotations about a vertical axis (see below).

4.2.2. Middle and Late Triassic. Unfortunately, we were not able to isolate a primary component in the Middle and Late Triassic sediments of the Xuyong region. Only a few paleopoles are available for this time range. Data retained (shown in Figure 20c and Table 4) are coming from many mostly deformed areas of south China. From the observations above, the poles from Nanjing of Jiangsu province [*Opdyke et al.*, 1986], Puxi area of Hunan

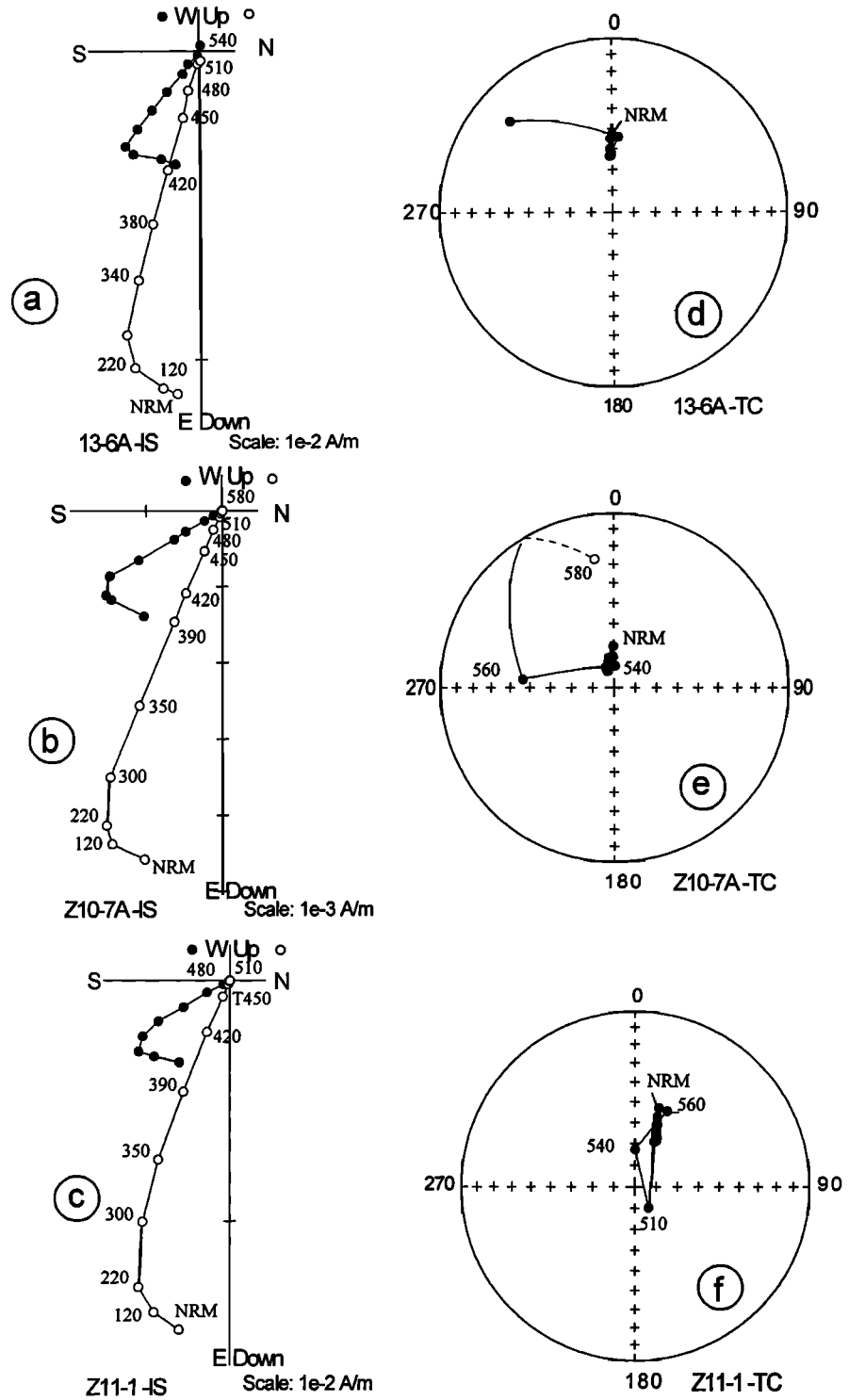

Figure 11. (a to c) Orthogonal vector projection of thermal demagnetization clearly showing two magnetic components before tilt correction, and (d to f) stereoplot of directional changes after tilt correction of Middle Triassic limestone samples. Symbols are same as in Figure 4.

provinces [*Huang and Opdyke*, 1996a] and central Hubei province [*Huang and Opdyke*, 1997] may represent the most autochthonous poles for this time slice (5 to 7 on Figure 20c). Indeed, the Permo-Triassic poles from Zhejiang [*Dobson et al.*, 1993; *Li and Wang*, 1989] close to Jiangsu poles cited above show no rotation with respect to data coming from western south China (Figure 20a). Other poles include data from the Guangxi (pole 3) and Hunan provinces (poles 1, 2, and 4, respectively) which have undergone important tectonic rotations. Poles from Yunnan region may have been rotated clockwise with respect to the stable Sichuan basin [*Yang and Besse*, 1993]. *Huang and Opdyke* [1996a] argued for a 13.5°±8.5° clockwise rotation of

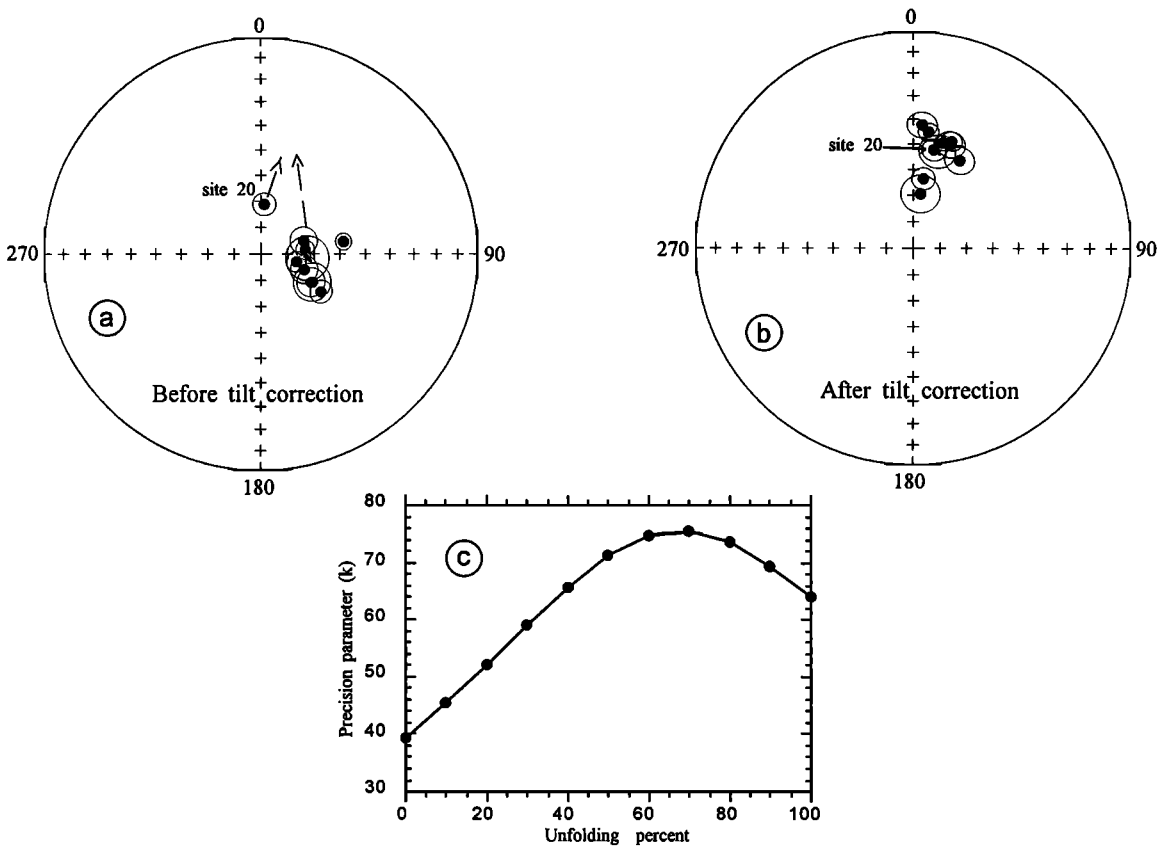

Figure 12. (a, b) Equal-area projection of the component B site-mean directions for the Middle Triassic before and after tilt correction. (c) Change of the precision parameter during unfolding insignificant at the 95% confidence level. However, the distribution of the site-mean directions is very similar to that of component B in the Early Triassic sediments. Dashed lines and arrows indicate the change of two groups of direction during the unfolding.

their Badong pole (1 on Figure 20c) with respect to their Sangzhi pole (2 on Figure 20c), both of them being clockwise rotated with respect to the Yangtze Craton. We agree with their analysis and notice that poles 1 and 2 and the nearby pole of *Dobson et al.* [1993] (3 on Figure 20c) are consistently rotated clockwise with respect to poles 5 and 6. *Huang and Opdyke* [1997] recently reported a new Middle Triassic pole from two different sections in the Hubei province. Although combined data from two sections pass the fold test, we note that the pole 7-1, yielded from the Maoping section, is consistent with, and located between pole 5 and 6. It is, however, significantly different from that of the Liujiatai section (pole 7-2)(Figure 20c). Instead of computing a

Table 2. Middle Triassic Site-Mean Directions and Corresponding Poles From the Xuyong Area (28°N/105.5°E) for Higher Temperature Component (300°-580°C)[a]

Site	*n*	In Situ		Tilt Corrected				Pole	
		D	*I*	*D*	*I*	*k*	α_{95}	λ(°N)	Φ(°E)
3	6	81.4	58.3	15.5	48.0	480.5	3.1		
13	9	122.2	63.1	8.0	63.3	146.1	4.3		
18	5	109.8	72.8	19.6	47.6	214.3	5.2		
19	5	102.5	76.4	19.5	46.3	400.8	3.8		
20	7	3.7	71.1	11.6	51.5	196.9	4.3		
Z10	6	118.8	67.9	7.3	69.2	86.5	7.2		
Z11	9	119.5	68.3	27.5	52.0	93.4	5.4		
Z16	8	84.6	73.3	7.4	44.7	239.5	3.6		
Z17	7	72.7	73.2	4.0	42.1	137.6	5.2		
Mean	9	95.2	72.4	13.7	51.8	63.9	6.5		
Mean[b]	9			23.9	62.2	75.5	6.0	65.3 *dp*=7.3°,	150.3 *dm*=9.3°

[a]For abbreviations see Table 1; [b]mean 70% unfolding level.

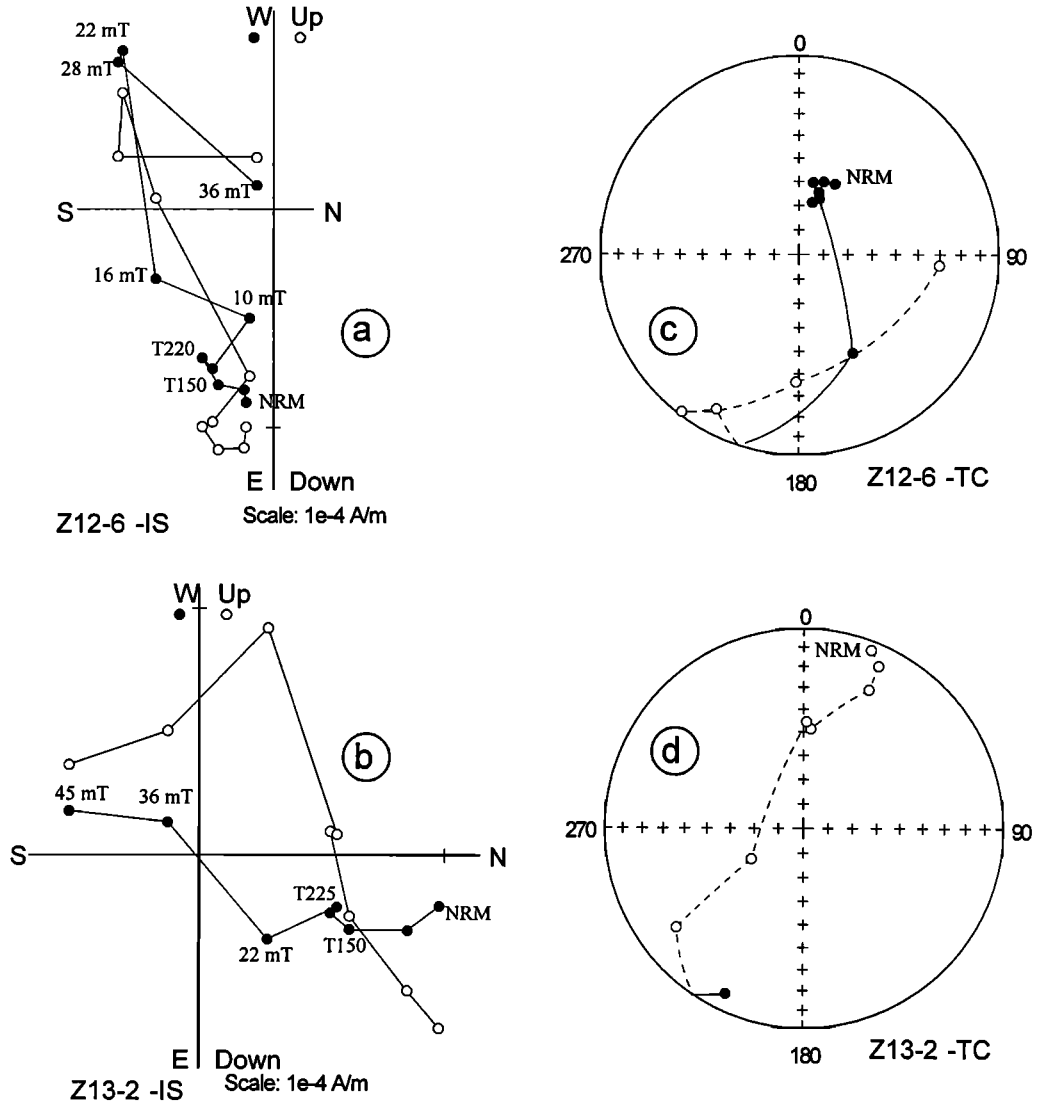

Figure 13. (a, b) Orthogonal vector projection of thermal demagnetization, and (c and d) stereoplots of NRM directions after tilt correction of Middle Triassic limestone samples. Symbols are same as in Figure 4.

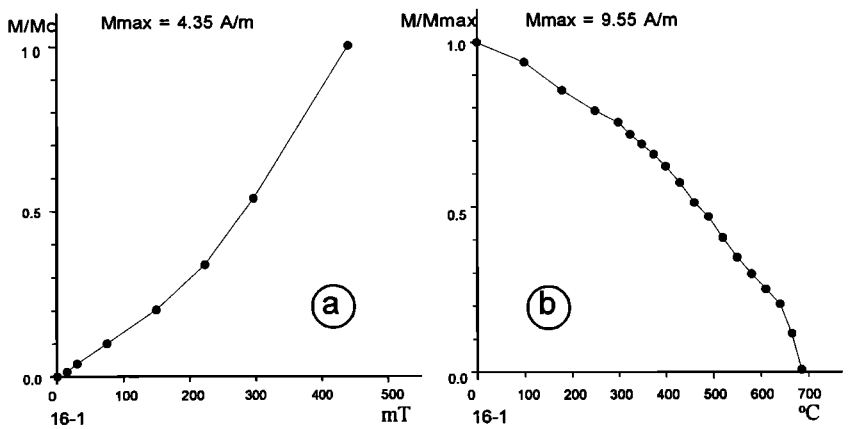

Figure 14. (a) Normalized isothermal remanent magnetization (IRM) acquisition curves, and (b) IRM thermal demagnetization showing unblocking temperatures around 690°C for the Early-Middle Jurassic red bed samples.

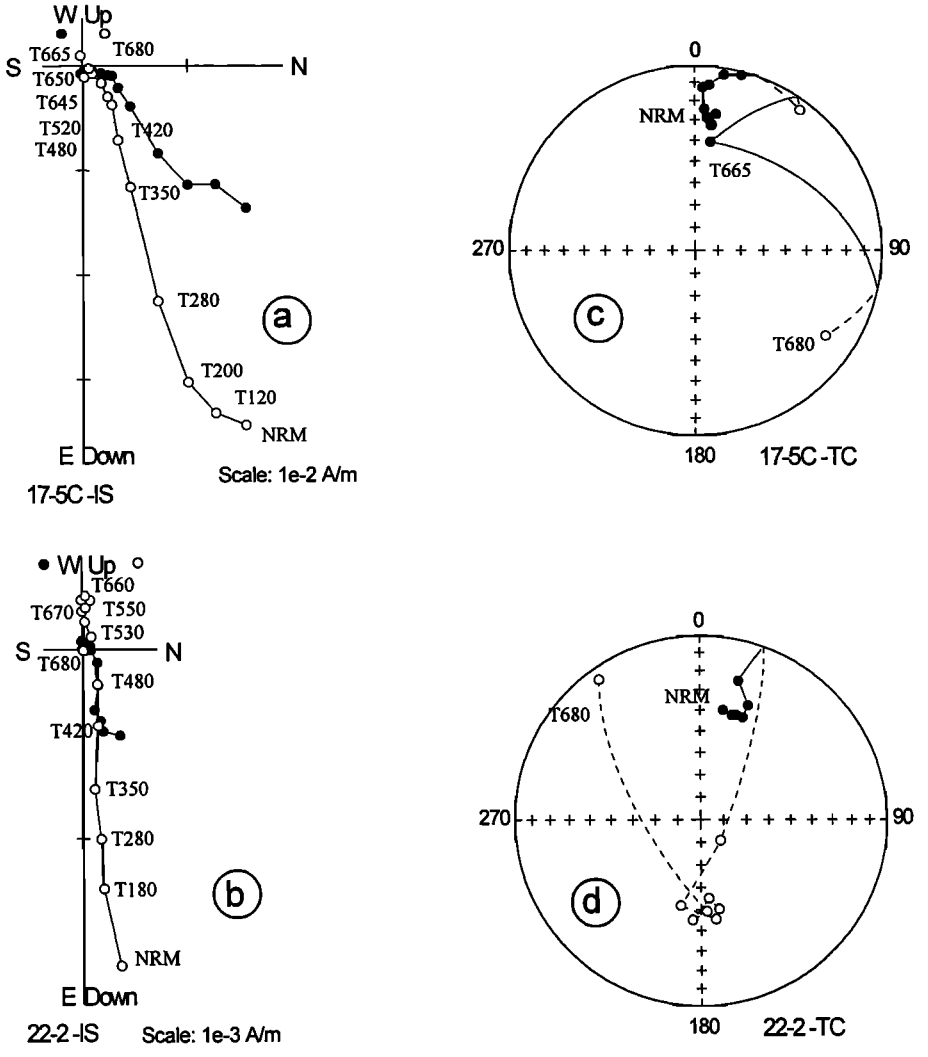

Figure 15. (a and b) Orthogonal vector projection of thermal demagnetization clearly showing two magnetic components after separating the present field overprint (in situ coordinates), and (c and d) stereoplots of magnetic direction changes (in tilt correction) of Early-Middle Jurassic red bed samples. Symbols are same as in Figure 4.

mean pole using classical Fisherian statistics, we have used a method which estimates the mean pole by a combination of pole directions and small circles [*Besse and Courtillot,* 1991]. The poles, which are suspect to come from areas rotated about vertical axes, are thus replaced by small circles the distance of which to the sampling sites is the paleocolatitude. By iteration, we then find a pole position with a Fisherian average of the pole directions and the nearest points on the small circles closest to this pole position. The method described by *McFadden and McElhinny* [1988] estimates the semicircle of confidence. Endpoints after iteration are shown in Figure 20c as solid triangles. Poles 1, 2, 4, and 7-2 after rotation fall close to the poles 5, 6, and 7-1, considered above to be situated in the most autochthonous regions of the Yangtze craton. Pole 3 is more remote but acceptable. The found pole (λ=42.7°N, ϕ=212.6°E, A_{95}=6.0°, Figure 20c) is statistically not different from previous Early Triassic poles (Figure 21).

4.2.3. Early-Middle Jurassic. Positive reversal and fold tests for the high-temperature component C of Xuyong series allow us to define a reliable Early-Middle Jurassic pole (light gray on Figure 20d, Table 3). Moreover, this pole originates as discussed above from sediment sequences situated in an autochthonous region. We may now compare it with other data of the same age. Two poles reported by *Huang and Opdyke* [1991] and *Zhu et al.* [1988] in the Sichuan and Yunnan provinces (poles 1 and 2 on Figure 20d) have clearly undergone local rotations related to the Xianshuihe strike-slip fault motion, as discussed by *Yang and Besse* [1993, Figure 9b]. *Gilder et al.* [1993b] also reported two early Jurassic poles from the Guangxi province of South China (poles 3 and 4). A comparison of these data with Cretaceous paleomagnetic poles of the Guangxi area, and also those of the cratonic Sichuan basin let them argue for local rotations in this area. They proposed to correct their Early Jurassic poles for local rotations caused by the Tertiary tectonic activity, expecting that both Cretaceous and Early Jurassic localities were similarly affected by faulting and rotation. Our Early-Middle Jurassic Xuyong pole (pole 5) is not different from their northernmost pole (pole 4 in Figure 20d) and does not need to be corrected. On the contrary, their Daling pole (pole 3) is clearly rotated and

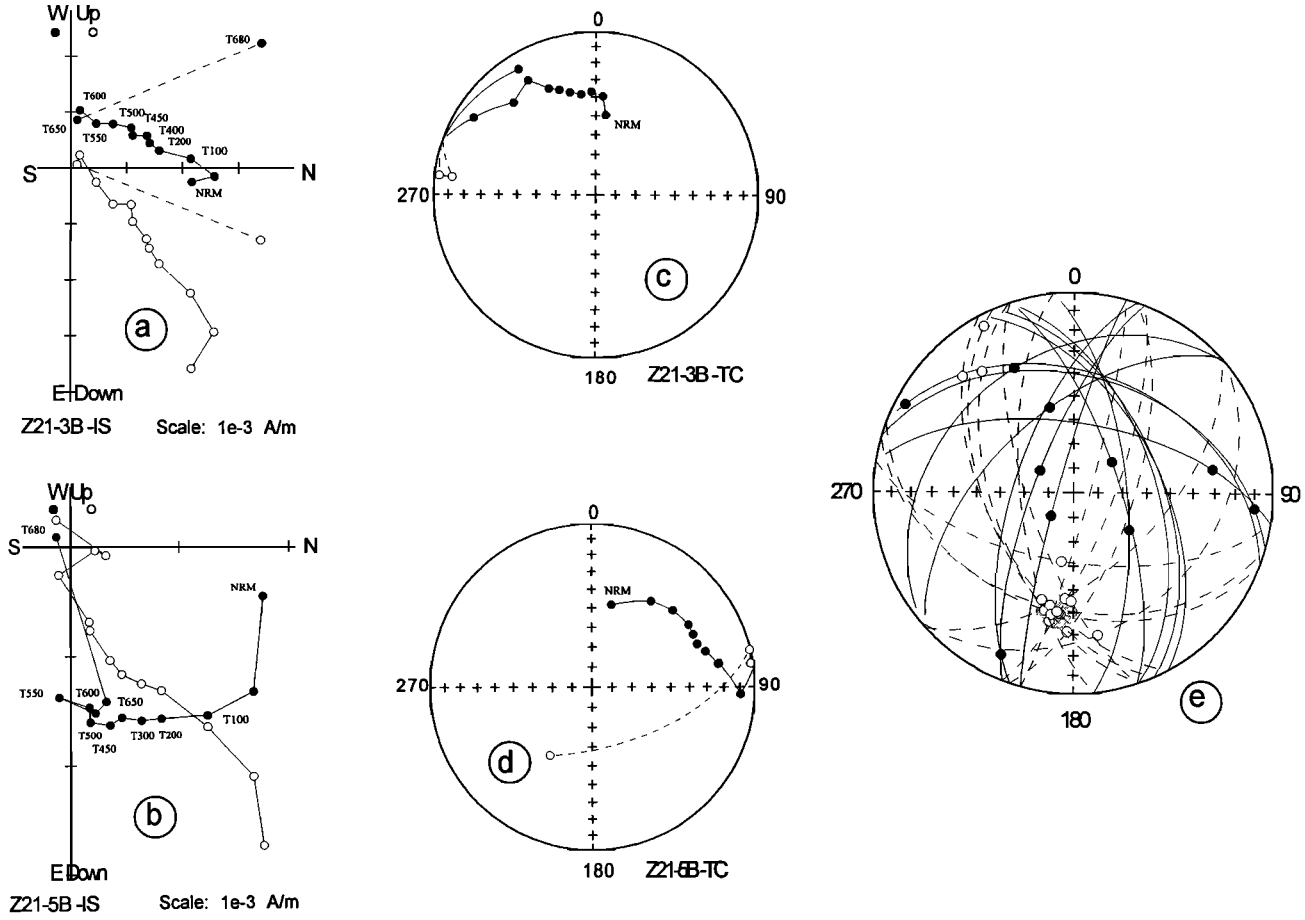

Figure 16. (a and b) Orthogonal vector projection of NRM thermal demagnetization showing an erratic directional changes after heating to 600°C. (c and d) Stereographic projections of NRM directions change along remagnetization great circles. (e) The site-mean direction for the Early-Middle Jurassic site Z21 calculated from the intersection of the great circles with limiting sector constraints. Symbols are same as in Figure 4.

underlines the important tectonic activity in this region. Figure 20d shows a very good grouping of the data after rotation of poles 1, 2, and 3. Using the method of small circle intersection yields a mean pole identical to our Xuyong pole alone. Clockwise rotation and northward motion of the South China Block are evidenced between the Middle/Late Triassic and the Early-Middle Jurassic.

4.2.4. Late Jurassic. Five Late Jurassic paleopoles of the SCB (Figure 20e) were reported from Zhejiang [*Lin et al.*, 1985], Sichuan [*Enkin et al.*, 1991; *Bai et al.*, 1998; *Yokoyama et al.*, 1999] and Yunnan [*Zhu et al.*, 1988]. We first notice that no relative significant rotation occurred between Sichuan and Zhejiang (3 and 4 on Figure 20e), as it has been also demonstrated for the P/T boundary poles. We have used the same small circle method to calculate the Late Jurassic mean pole, since the pole from the Yunnan region was affected by local rotations [*Yang and Besse*, 1993]. The mean pole obtained has a fairly small A_{95} (8.6°) and can not be distinguished from the above mentioned Early and Middle Jurassic pole nor from the Early Cretaceous one (see below).

4.2.5. Cretaceous and Paleocene. Extensive paleomagnetic studies of Cretaceous strata were carried out in south and north China during the last decade (see review by *Yang et al.* [1995]). In addition to these data, *Wu et al.* (1993) and *Gilder and Courtillot* [1997] recently reported two Early-Middle Cretaceous poles from the Shaanxi and Anhui provinces on the NCB. Except the paleopoles from the central Yunnan basin, Guangxi and Hainan areas, most SCB poles cluster very well. The mean Early Cretaceous paleopoles for the NCB and SCB are 76.4°N, 208.8°E, A_{95}=5.1° and 74.3°N, 225.2°E, A_{95}=5.5°, respectively. These two poles are statistically indistinguishable at the 95% level according to the test of *McFadden and McElhinny* [1990]. North and south China were a single block. Thus the poles for the two blocks were compiled together (λ=76.2°N, ϕ=211.2°E, A_{95}=3.7°, N=10) (Table 4).

No new poles have been added for the Late Cretaceous and the resulting definition has an A_{95} of nearly 10°. The distribution of individual poles shows that the two poles of *Enkin et al.* [1991] in Sichuan province and *Hsü et al.* [1987] in Guangdong are situated close to Paleocene poles of south China. Indeed, a series of Paleocene poles were reported by *Ge et al.* [1994]. These poles are more or less dispersed along a small circle centered on the sampling site. Despite this dispersion, the mean pole is well defined with an A_{95} of only 7.8°.

4.2.6. Main features of the Mesozoic APWP for the SCB.

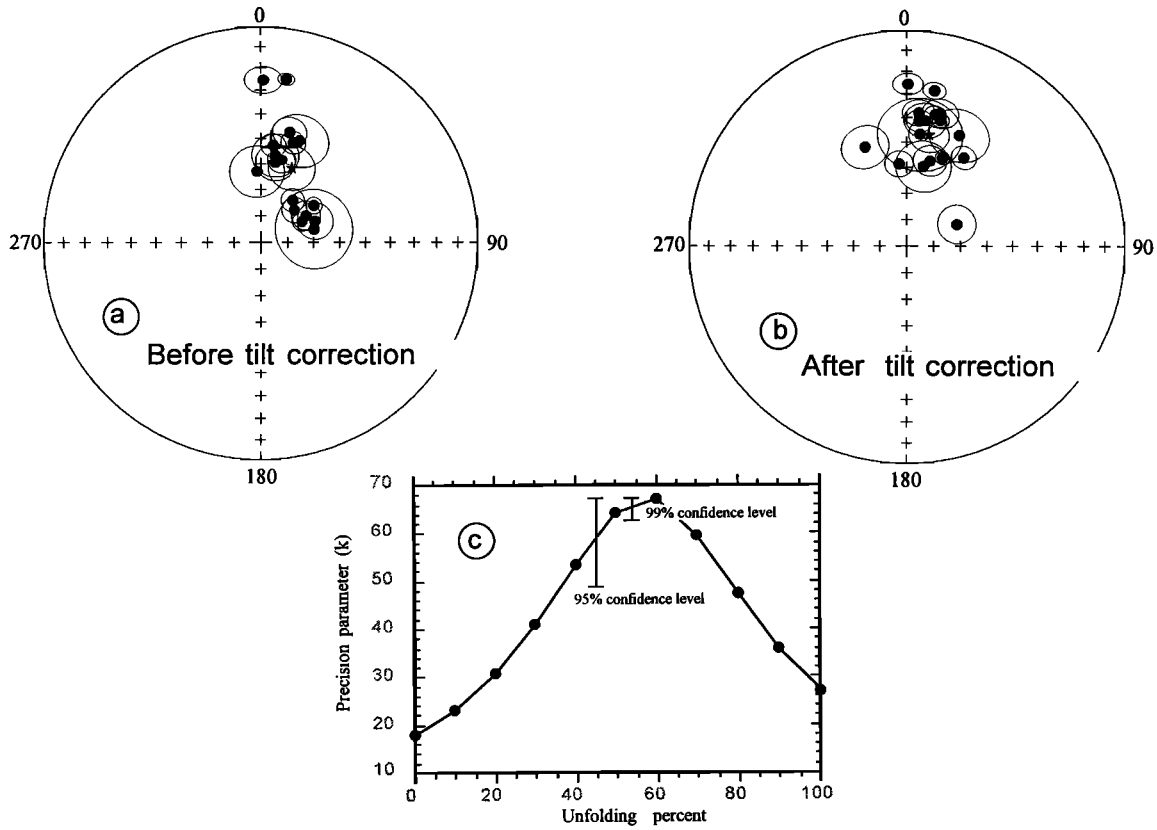

Figure 17. (a, b) Equal-area projection of component B site-mean directions for the Early-Middle Jurassic sediments before and after tilt correction, and (c) a significant maximum of the precision parameter (k) at 60% unfolding with the 95% and 99% confidence levels displayed.

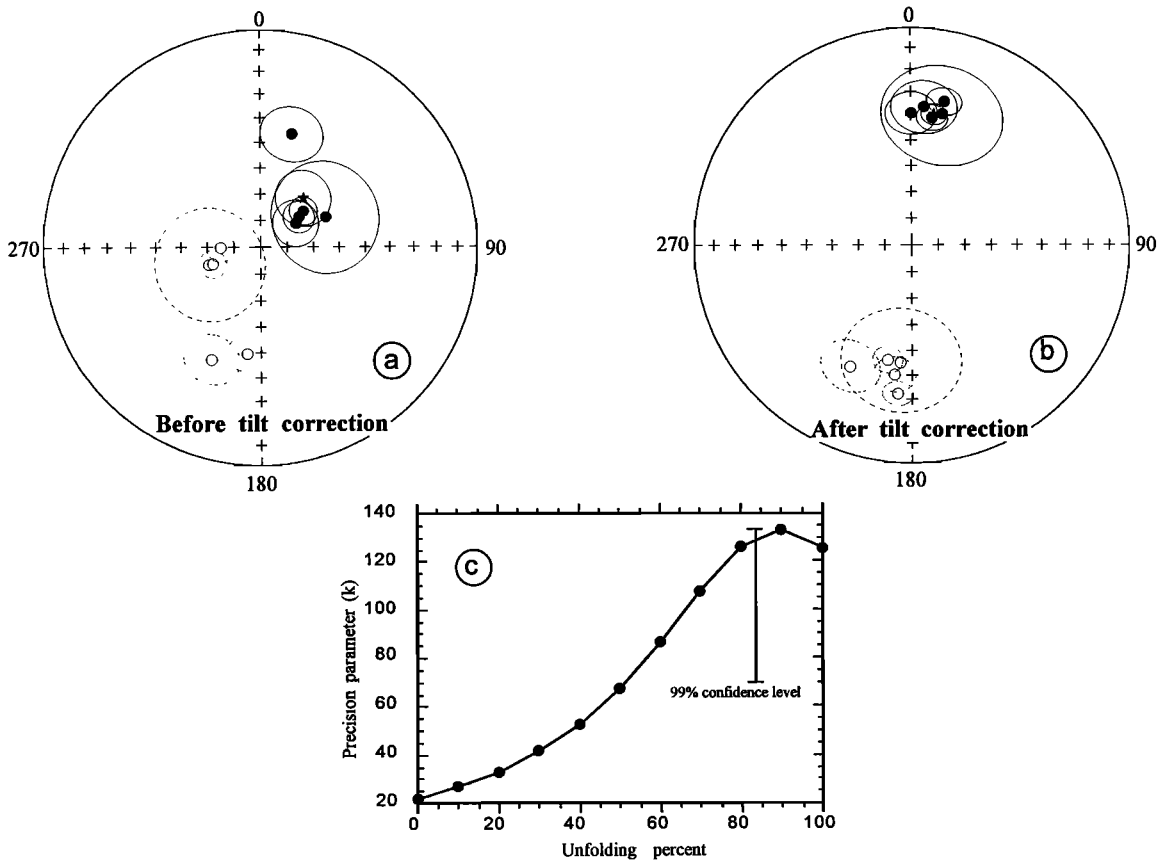

Figure 18. (a, b) Equal-area projection of the component C site-mean directions for the Early-Middle Juriassic sediments before and after tectonic tilt correction, and (c) the change of the precision parameter (k) during unfolding up to 100%.

Table 3. Lower/Middle Jurassic Site-Mean Directions and Corresponding Poles From the Xuyong Area (28°N/105.5°E)[a]

Site	*n*	In Situ		Tilt -Corrected				Pole	
		D	*I*	*D*	*I*	*k*	α_{95}	λ(°N)	Φ(°E)
				Middle Temperature Component B (200°-500°C)					
Z14	8	55.1	65.4	14.6	39.3	329.2	3.1		
Z15	5	75.7	69.2	6.6	46.4	27.6	14.8		
Z19	19	45.6	72.3	0.4	25.6	49.8	4.8		
Z20	16	18.0	49.6	5.6	41.1	68.4	4.5		
Z21	14	14.7	46.0	14.1	36.6	43.6	6.1		
Z22	7	10.2	58.9	65.9	69.6	71.3	7.2		
Z23	12	0.9	25.4	14.9	56.2	53.0	6.0		
1	5	7.3	52.4	32.3	49.7	284.7	4.5		
16	10	59.1	70.1	5.1	37.8	77.8	5.5		
17	7	68.2	67.9	8.2	40.7	71.0	7.2		
22	10	62.8	72.6	12.0	37.5	185.9	3.6		
23	6	37.0	70.0	10.0	27.5	330.7	3.7		
24	4	9.4	56.2	337.3	48.6	117.6	8.5		
25	5	13.9	57.5	354.6	58.4	229.2	5.1		
26	6	20.8	48.0	24.9	42.6	40.8	10.6		
27	4	356.9	62.9	11.5	58.9	85.2	10.0		
28	8	8.9	24.2	21.7	53.6	444.6	2.6		
Mean	17	22.5	59.2	-	-	17.9	8.7		
Mean	17	-	-	11.1	46.2	26.9	7.0		
Mean[b]	17			13.9	51.9	67.1	4.4	77.2 *dp*=4.1°,	171.4 *dm*=6.0°
				Higher Temperature Component C (500°-680°C)					
Z14	9	50.1	68.9	9.5	40.2	94.2	5.3	80.0	224.1
Z15	4	251.3	-69.5	185 6	-45.0	36.4	21.0	84.8	210.3
Z19	20	250.7	-71.0	185.6	-32.1	42.7	5.1	78.2	258.4
Z20	9	15.8	44.8	5.5	36.1	24.2	11.1	80.6	252.1
Z21	13	187.4	-49.2	187.8	-39.8	38.8	7.2	81.1	231.1
16	8	56.0	74.0	0.2	38.9	43.7	8.8	84.0	283.7
17	5	65.3	62.7	13 5	37.8	16.6	20.7	76.0	221.5
22	10	269.2	-75.1	192.1	-45.2	97.2	5.3	79.2	199.5
23	7	52.0	71.7	13.2	32.6	111.0	5.8	74.1	232.9
26	5	203.9	-43.0	207.2	-37.4	71.5 1	10.4	64.3	205.4
Mean	10	41.4	65.4	-	-	22.1	10.5		
Mean	10	-	-	10.0	38.7	125.3	4.3	79.0	227.5
Mean							4.5	79.1	226.9
Mean +	5			8.5	37.2	230	5.1		
Mean -	5			191.7	-40.2	82.2	8.5		

[a]For abbreviations see Table 1. [b]mean at 60% unfolding level. (1) Reversal test positive at 95% confidence level (B class): $\gamma_0 = 3.9° < \gamma_{\text{critcal value}} = 8.9°$ following *McFadden and McElhinny* [1990], and (2) fold test for the higher temperature component C, *McElhinny*'s[1964] method, *ks/kg*=5.7 > *F*(18,18)=3.13 at 99% confidence level.

The difference between our new Mesozoic APWP and those reported previously [*Lin et al.*, 1985; *Enkin et al.*, 1992b; *Wang et al.*, 1993] is the determination of paleopoles for the Permo-Triassic boundary, the Middle Triassic, and the Early-Middle Jurassic. These poles are generally obtained from widely separated sampling localities and characterized by fold and reversal tests. The Mesozoic APW loop proposed by *Wang et al.* [1993] is based on their folding-associated pole. This remagnetization proposition is rejected by *Huang and Opdyke* [1996b, 1997] and by this study.

Figure 21 shows the successive mean pole positions (Table 4). The Late Permian, P/T boundary, and Early Triassic means are statistically different at the 95% probability level and form a track. However, such a track may represent polar wander or some random combination of poles computed from tectonically rotated sites [*Enkin et al.*, 1992b]. Another potential problem is connected with changes in the strike of the folds of the Sichuan basin, which appear to be a remarkable feature of this region [*Enkin*, 1990]. *Steiner et al.* [1989] have associated the change in strike of the folds from N10° to N40° between the sites of north central and southern parts of the eastern regions of the Sichuan basin with similar changes in the declination (however, with a significantly smaller amplitude of around 15°). *Steiner et al.* [1989] therefore concluded that a major deformation episode did bend the Sichuan basin at a crustal scale ("oroclinal bending") at same time during the Late Cretaceous or Tertiary. The Middle Triassic paleomagnetic poles in the Hunan province derived from Badong and Sangzhi areas (Figure 20c, poles 1 and 2) by *Huang and Opdyke* [1996b] are rotated with respect to the Yangtze Craton and also show a correlation between declinations and fold trends.

However, our new data question such a model. We have plotted the declinations (and their associated error bars) with respect to the strike of the folds for three age windows (the Permo-Triassic boundary, the Early Triassic, and the Middle Triassic). In some studies where the bedding attitude was not provided, the strike has

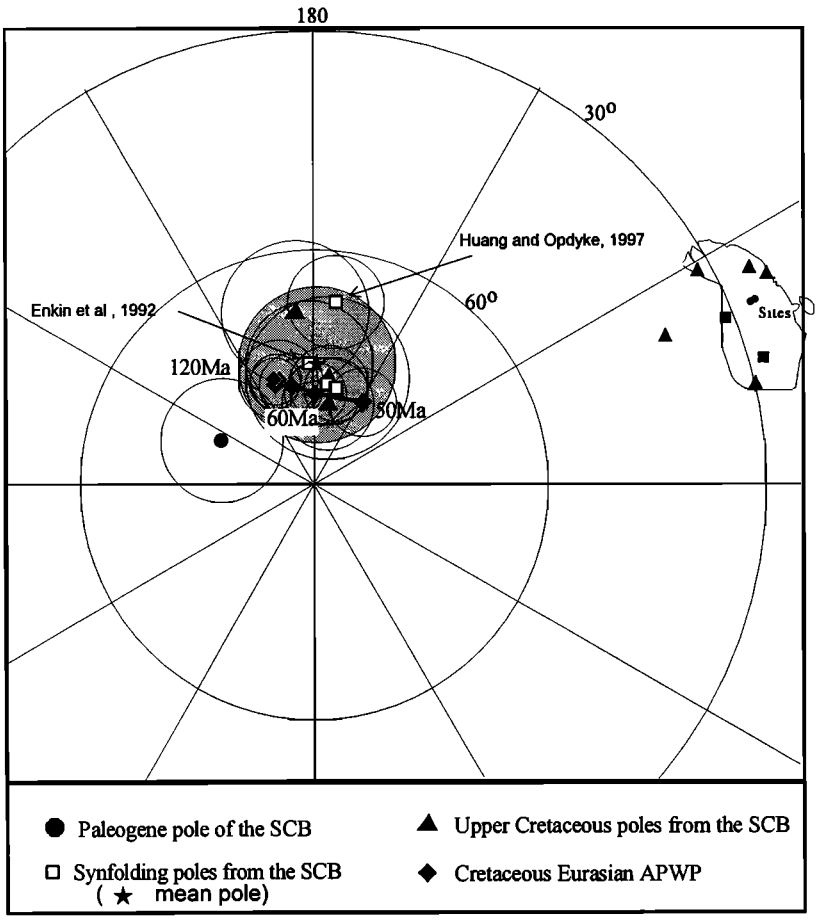

Figure 19. Lower Triassic and Lower Jurassic synfolding remagnetized poles (open squares) compared with Late Cretaceous poles (solid triangles) and Early Tertiary poles (solid circles) from south China and Eurasia (diamonds) [*Besse and Courtillot,* 1991]. Remagnetized poles reported by *Enkin et al.* [1992a] and *Huang and Opdyke* [1997] are also shown. The sampling localities are marked on the map of south China: solid squares for the remagnetized Triassic, triangles for the Cretaceous, and small dots for the Tertiary.

been approximated as the pole of the small circle passing through the corrected and uncorrected directions.

In Figure 22a, significantly different declinations from the Puxi and Badong areas with similarly striking fold axes appear to contradict the oroclinal bending hypothesis. Huang and Opdyke [1997] also recently obtained in the central Hubei province a new Middle Triassic pole from two sections with different bedding strike directions (Maoping section with a N335°W trending fold and Liujiatai section with a N75°E bedding strike direction). The paleodeclination from the Maoping section is statistically indistinct from that of the Puxi section (Figure 22a, S-T2-2) and inconsistent with that calculated for the Liujiatai section. We thus feel that the Liujiatai section more likely suffered a local counterclockwise (CCW) rotation (>15°) with respect to the Yangtze block, related to peculiar thrust faulting in the area.

Moreover, the declinations are nearly identical (their error bars always intersect) in each of the two oldest time windows (Figures 22b and 22c). They also appear to be independent from the fold azimuth of the considered region. The paleodeclination obtained from the NEE-SWW (around 80°) trending syncline of our study (Figure 22b, S-T1-2) in the southern part of the Sichuan basin is also coherent with the other results. This observation is also supported by the Early Triassic paleomagnetic studies from the Wulong, Shujiang, and Linshui areas with NE-SW striking fold axes [*Heller et al.,* 1995] (Figure 22b, S-T1-9). Thus the declinations do not appear to be correlated with tectonic structures and hence do not suggest oroclinal bending.

The distribution of paleomagnetic sites in a wide area on the Yangtze block and the associated pole directions stand for the motion of a "rigid" Sichuan block (Figure 22c). A fast phase of counterclockwise rotation of 22.3°± 9.5° (at reference site 28°N, 105°E) thus occurred from the Late Permian until the Early Triassic. The Middle Triassic pole is statistically indistinguishable from the Early Triassic one. This phase is followed by a clockwise 35°±8° rotation at the same reference site, which stopped during the Early and Middle Jurassic. This part of the track is not well documented since Late Triassic paleomagnetic studies failed to isolate primary components. The only information is given by the Yunnan pole of *Zhu et al.* [1988], situated on the track close to the Middle Triassic pole, but being suspect of local rotations [*Yang and Besse,* 1993].

The Late Jurassic, Cretaceous, and Paleocene poles of the SCB

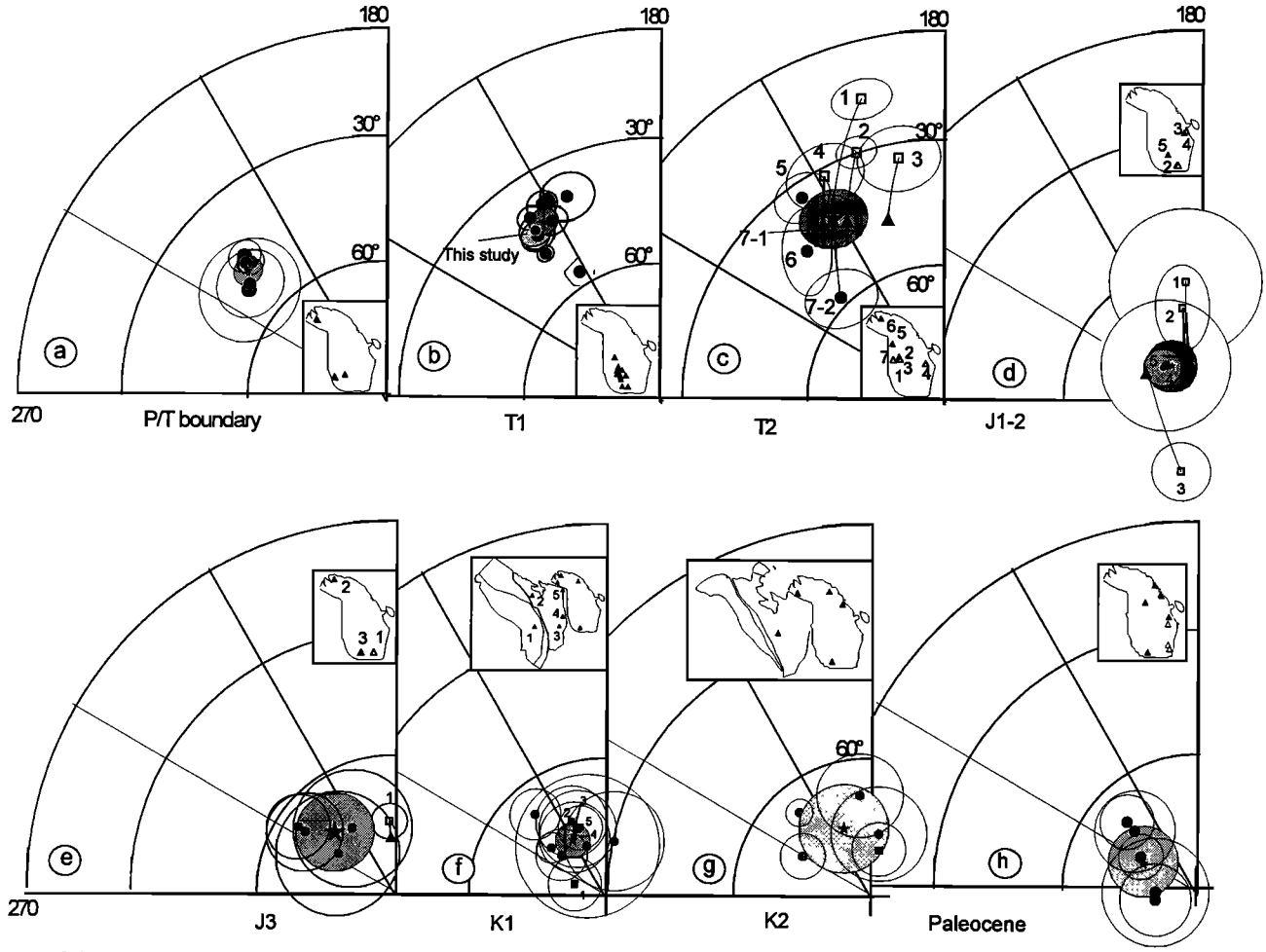

Figure 20. Stereographic north polar projection of paleopoles from the South China Block for (a) the Permo-Triassic boundary (P/T), (b) the Early Triassic (T1), (c) the Middle Triassic (T2), (d) the Early-Middle Jurassic (J1-2), (e) the Late Jurassic (J3), (f) the Early Cretaceous period (K1), (g) the Late Cretaceous, and (h) the Paleocene (solid circles for the poles of the SCB, squares for the poles of the NCB). Paleopoles which suffered local rotations and that after iteration are shown as open squares and solid triangles, respectively. Each mean pole position is indicated by a star with a 95% half angle of confidence (light gray) (see text and Table 4). The sampled locations are indicated in the inset with a number which corresponds to their pole.

are within the common intersection of their 95% domain of confidence (Figures 20e-20h). The stationary nature of these paleopoles is remarkable during these periods, as noted by *Courtillot and Besse* [1986] and *Enkin et al.* [1992b].

4.3. Collision Timing Between the North and South China Blocks

Previous paleomagnetic studies have already addressed the collision history of the NCB and SCB [*Lin et al.*, 1985; *Opdyke et al.*, 1986; *Zhao and Coe*, 1989; *Zhao et al.*, 1990; *Yang et al.*, 1991, 1992; *Enkin et al.*, 1992b; *Huang and Opdyke*, 1996b; *Gilder and Courtillot*, 1997]. They concluded that the two blocks have been welded together after the Triassic and before the Late Jurassic. We may now compare the APWPs of these two blocks to refine the history in the light of the new data we have obtained.

Mesozoic paleopoles for the North China Block mainly come from the Ordos Basin [*Yang et al.*, 1991, 1992]. Additional paleomagnetic data have been obtained by several authors [*Ma et al.*, 1992; *Zheng*, 1992; *Tan et al.*, 1995; *Embleton et al.*, 1996; *Gilder and Courtillot*, 1997] from other places. The APWP obtained in the Ordos basin by *Yang et al.* [1991, 1992] is confirmed by these data, and even strengthened, since the NCB has proved to behave as a rigid block. We have integrated the new data (see Table 4) to better constrain the APW path of this block. The agreement between poles is excellent for each of the time windows (Figure 23) and yields the path displayed on Figure 21.

The motion of the North China Block with respect to the Earth rotation axis can be summarized as follows: a period of slow counterclockwise rotation (12° ± 6°/31 Ma) with a northward component of motion (10°± 6°/31 Ma calculated at the reference site 35°N, 110°E), is first observed from the Late Permian to Middle Triassic. It is then followed by a fast rotation (38.2° ± 6.4°/40 Ma) from the Late Triassic to Middle Jurassic. The same standstill as for the SCB is also shown during the Late Jurassic and the Cretaceous.

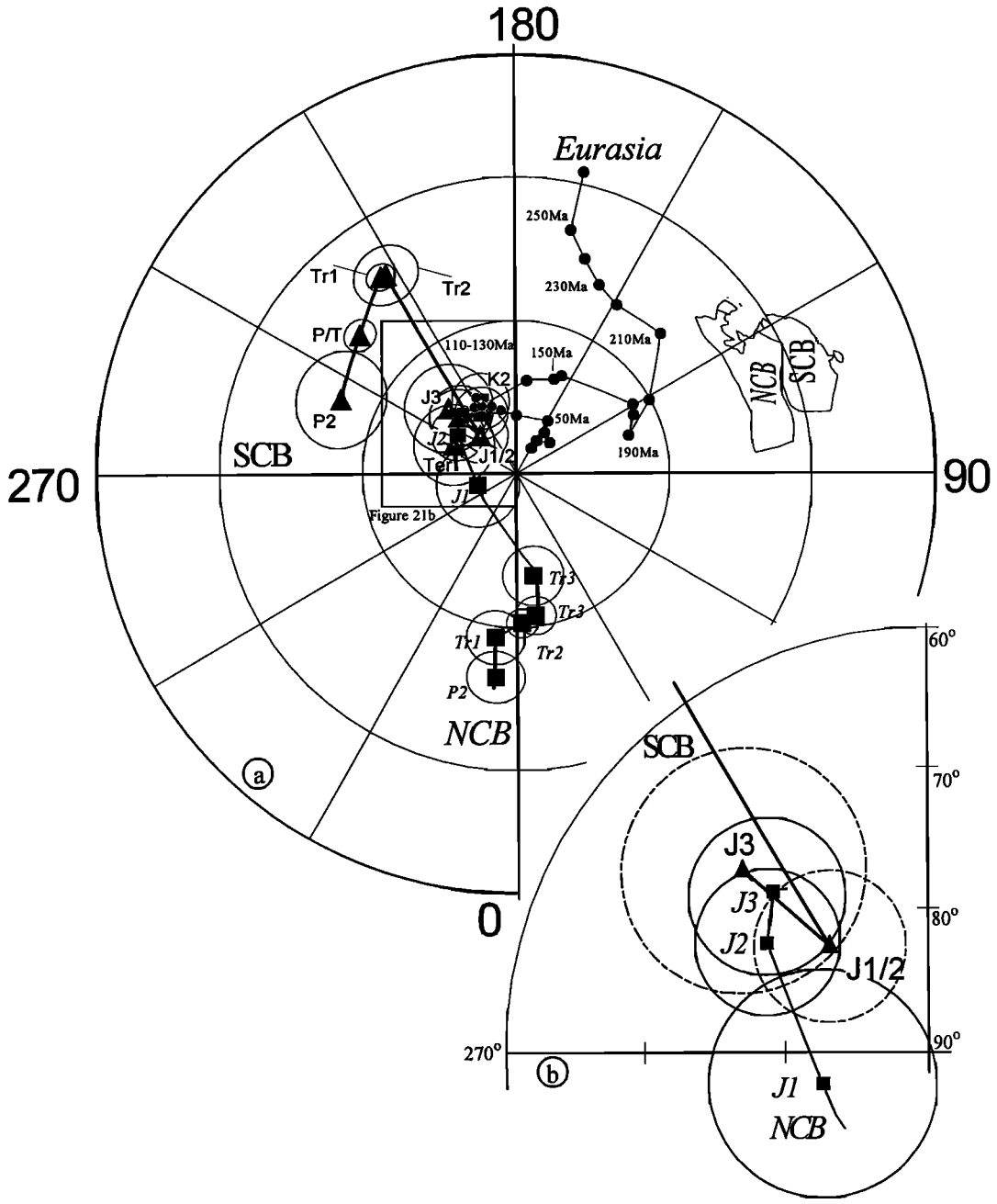

Figure 21. (a) The Mesozoic APW path of the South China Block in stereographic projection (solid triangles). P2, Late Permian; P/T, Permo-Triassic boundary; T1, Early Triassic; T2, Middle Triassic; T3, Late Triassic. The Mesozoic APW paths from the North China Block (solid squares) and Eurasia (dots) [*Besse and Courtillot,* 1991] are also presented for further comparison (see text and Table 4). (b) Enlarged stereoplot of the Jurassic poles from the NCB and SCB.

The comparison between the NCB and SCB APWPs from Late Permian to Late Triassic clearly shows that the two tracks follow similar trends, indicating minor relative motion during this time. This period is then followed by opposite rotations of the two blocks with comparable amplitude. At face value, an angular distance of 10.5° ± 9.6° between the Early and Middle Jurassic NCB poles may mark the slow down of the fast counterclockwise rotation of this block (Figure 23). A similar standstill to that of SCB is then displayed during the Late Jurassic and the Cretaceous.

We now compare the NCB and SCB APWPs of Figure 21. These paths are clearly separated from Permian times to Early Jurassic, when they become indistinct. After a phase of slow common counterclockwise rotation at a nearly constant latitude ending by the Middle Triassic, the scissor-like collision process [*Zhao and Coe,* 1987] was performed with a fast counterclockwise rotation of the North China Block with respect to south China.

Mattauer et al. [1991] argued that the collision between the

Table 4. All Mesozoic and Upper Permian Poles From the North and South China Blocks[a]

Block	Site Location		Pole Position		A_{95}	References
	°N	°E	λ(°N)	Φ(°E)	(*dp/dm*)	
			Asian Plate (NCB+SCB+Mongolia)			
Early Tertiary						
S	27.0	112.5	68.9	227.0	6.0	*Ge et al.* [1994]
S	27.0	112.5	76.1	241.6	5.0	*Ge et al.* [1994]
S	27.0	112.5	76.1	228.0	9.0	*Ge et al.* [1994]
S	27.0	112.5	81.0	277.8	12.0	*Ge et al.* [1994]
S	27.0	112.5	80.6	287.8	8.0	*Ge et al.* [1994]
Mean Paleocene	*N*=5		76.8	243.9	7.8	Fisherian mean
Late Cretaceous						
N	40.1	112.9	79.6	170.1	5.8	*Zheng et al.* [1991]
S	25.0	116.4	67.9	186.2	9.2	*Hu et al.* [1990]
S	32.0	119.0	76.3	172.6	10.3	*Kent et al.* [1987]
S	23.0	115.0	66.0	221.5	2.3/4.2	*Hsu* [1987]
S	30.0	102.9	72.8	241.1	4.1/7.4	*Enkin et al.* [1991]
S[b]	26.6	102.4	78.9	186.6	5.5	*Zhu et al.* [1988]
S[b]	26.5	102.3	81.9	220.9	7.1	*Huang and Opdyke* [1992]
S[b]	26.0	117.3	65.1	207.2	5.0	*Gilder et al.* [1993a]
S[b]	23.1	113.3	56.2	211.5	3.9	*Gilder et al.* [1993a]
S[b]	22.7	108.7	79.4	7.1	10	*Gilder et al.* [1993a]
Mean K1-2	*N*=10		74.3	205.1	5.5	small circles
	N=5		74.3	202.4	9.9	Fisherian mean (without pole)[b]
Cretaceous (K1-2)						
N	37.2	105.0	74.5	203.4	8.2	*Wu et al.* [1993]
N	31.6	116.0	74.5	201.0	4.7	*Gilder and Courtillot* [1997]
Early Cretaceous						
N	35.0	108.0	75.8	208.7	7.5	*Ma et al.* [1993]
M	45.4	107.6	72.5	205.3	7.6	*Pruner* [1992]
M	42.0	119.2	82.9	249.5	5.7	*Zhao et al.* [1990]
S[b]	25.9	101.7	64.6	199.6	3.3	*Otofuji et al.* [1998]
S	26.0	117.2	66.9	221.4	5.4	*Zhai et al.* [1992]
S[b]	26.8	102.5	69.0	204.0	4.3	*Huang and Opdyke* [1992]
S	29.7	120.3	77.1	227.6	5.5	*Lin et al.* [1985]
S	30.0	102.9	74.5	229.0	3.2	*Enkin et al.* [1991]
S	30.0	103.0	78.6	201.0	15.3	*Zhuang et al.* [1988]
S	22.2	114.2	78.2	171.9	10.6	*Chan* [1991]
S[b]	22.7	108.7	86.5	26.4	6.8	*Gilder et al.* [1993a]
S[b]	18.9	109.4	83.2	143.0	9.8	*Li et al.* [1995]
Mean K1-(2)	*N*=14		76.4	207.8	3.1	small circles
NCB	*N*=5		76.4	208.8	5.1	
SCB	*N*=5		74.3	225.2	5.5	
NCB and SCB	*N*=10		76.2	211.2	3.7	Fisherian mean
			South China Block			
Late Jurassic						
S	29.4	120.0	73.0	213.7	12.6	*Lin et al.* [1985]
S	29.9	102.9	74.6	235.3	13.2	*Enkin et al.* [1991]
S[b]	26.7	102.4	74.2	185.7	3.8	*Huang and Opdyke* [1991]
S	32.1	106.2	66.6	236.4	8.5	*Bai et al.* [1998]
S	31.8	106.7	64.7	236.0	7.0	*Yokoyama et al.* [1999]
Mean Late Jurassic	*N*=5		71.8	224.8	8.6	small circles
Early-Middle Jurassic						
S	28. 5	105.0	79.1	226.9	4.5	this study
Early Jurassic						
S[b]	26. 8	102.3	63.8	188.2	16.1	*Huang and Opdyke,* [1991]
S[b]	26. 8	102.3	69.4	192.4	5.8/9.4	*Huang and Opdyke,* [1991]
S	22.6	108.5	79.0	225.8	14.0	*Gilder et al.* [1993b]
S[b]	22.0	108.7	74.2	343.8	6.3	*Gilder et al.* [1993b]
Mean Early-Middle Jurassic	*N*=5		79.9	221.8	5.3	small circles
Middle Triassic						
S-T2-1[b]	23.6	107.2	32.2	208.7	7.9	*Gilder et al.* [1995]
S-T2-2	32.0	119.0	44.8	223.6	5.4/10	*Opdyke et al.* [1986]

Table 4. (continued)

Block	Site Location		Pole Position		A_{95}	References
	°N	°E	λ(°N)	Φ(°E)	(*dp/dm*)	
S-T2-3[b]	31.0	110.4	16.6	195.8	5.5	*Huang and Opdyke* [1996b]
S-T2-4[b]	29.4	110.2	29.8	200.0	4.0	*Huang and Opdyke* [1996b]
S-T2-5	29.7	113.9	33.8	215.8	5.8	*Huang and Opdyke* [1996b]
S-T2-6	31.4	111.7	50.5	218.8	5.8	*Huang and Opdyke* [1997]
S-T2-6-1	31.4	111.7	42.3	213.9	3.7/6.8	Maoping section
S-T2-6-2[b]	31.4	111.7	57.2	225.8	5.5/10	Liujiatai section
Early Middle Triassic						
S-T2-7[b]	29.5	110.0	34.0	191.0	8.2	*Dobson and Heller* [1993]
Mean (Early-)Middle Triassic	*N*=8		42.7	212.6	6.0	small circles
	N=3		40.4	217.6	10.6	Fisherian mean (without pole)[b]
Early Triassic						
S-T1-1	28.6	106.9	44.5	217.8	2.7/5.3	*Opdyke et al.* [1986]
S-T1-2	28.0	105.5	44.1	217.2	4.9	this study
S-T1-3	29.9	106.3	38.7	211.8	3.2./6.3	*Steiner et al.* [1989]
S-T1-4	29.5	105.0	43.3	211.7	3.3/6.4	*Enkin et al.* [1992a]
S-T1-5	30.0	107.0	39.8	216.2	2.7/5.3	*Enkin et al.* [1992a]
S-T1-6	29.6	103.4	48.8	218.7	1.8/3.6	*Ma and Zhang* [1989]
S-T1-7	28.2	103.0	56.8	212.6	3.2/5.9	*Zhu et al.* [1988]
S-T1-8	29.5	110.0	39.8	205.1	5.7	*Dobson and Heller* [1993]
S-T1-9	29.3	107.7	44.3	217.4	3.5	*Heller et al.* [1995]
S-T1-10	32.1	106.2	42.5	214.6	8.5	*Bai et al.* [1997]
(Permo-) Early Triassic						
S-T1-11	30.0	106.3	38.5	209.8	1.7/3.3	*Steiner et al.* [1989]
Mean Early Triassic	*N*=11		43.8	213.8	3.5	this study
	N=10		42.5	213.9	2.7	this study (without *Zhu et al.* [1988])
Permo-Early Triassic boundary						
S-PT-1	31	119.7	51.1	230.3	7.4	*Li and Wang* [1989]
S-PT-2	31	119.7	51.8	232.1	11.2	*Dobson et al.* [1993]
S-PT-3	32.4	105.5	47.9	225.1	2.8/5.0	*Heller et al.* [1988]
S-PT-4	29.6	105.6	45.8	225.2	3.5/7.0	*Steiner et al.* [1989]
S-PT-5	32.4	105.5	47.2	226.3	2.1/4.2	*Steiner et al.* [1989]
Mean Permo-Triassic	*N*=5		48.8	227.7	3.1	this study
Mean Upper Permian	*N*=6		52.7	246.4	9.1	*Enkin et al.* [1992b]
		North China Block				
Late Jurassic						
N	31.6	116.0	74.4	222.8	5.9	*Gilder and Courtillot* [1997]
Middle Jurassic						
N	31.6	116.0	72.9	254.7	6.4	*Gilder and Courtillot* (1997)
N	36.7	109.2	74.3	232.8	4.5	*Yang et al.* [1992]
N	37.0	109.0	73.1	251.9	15.7	*Frost* [1994]
N	40.1	112.9	76.2	199.9	8.3	*Zheng* et al. [1991]
N	38.6	112.0	76.1	214.6	13.0	*Fang et al.* [1988]
N	37.0	109.0	80.3	249.4	4.0	*Cheng et al.* [1988]
Mean Middle Jurassic	*N*=6		76.4	234.8	5.1	this study
Early Jurassic						
N	36.2	109.3	82.6	284.1	8.0	*Yang et al.* [1992]
Late Triassic						
N	35.4	109.6	62.3	7.7	3.8	*Yang et al.* [1991]
N	35.1	109.0	70.1	9.4	5.8	*Wu et al.* [1993]
Middle Triassic						
N	35.2	109.2	63.8	353.7	9.0	*Yang et al.* [1991]
N	35.2	109.2	57.3	1.9	5.0	*Yang et al.* (1991)
N	39.0	112.0	60.0	358.8	9.7	*Ma et al.* [1992]
N	38.0	110.4	59.6	7.3	5.5	*Zheng* [1992]
N	36.2	110.8	64.0	6.0	4.0	*Tan et al.* [1995]
N[c]	38.5	112.1	47.6	18.3	3.0	*Fang et al.* [1988]

Table 4. (continued)

Block	Site Location		Pole Position		A_{95}	References
	°N	°E	λ(°N)	Φ(°E)	(*dp/dm*)	
N	36.2	112.1	60.8	10.4	4.0	*Tan et al.* [1995]
N[c]	35.0	109	49.1	12.5	3.7	*Cheng et al.* [1988]
N	35.1	109.1	60.3	355.3	6.0	*Wu* [1988]
Mean (Early-)Middle Triassic						
	N=9		58.3	5.7	4.7	this study
	N=7		61.0	2.0	2.9	(without poles)[c]
Early Triassic						
N	35.5	110.2	61.9	348.3	3.8	*Yang et al.* [1991]
N	34.9	109.0	58.0	354.1	5.0	*Ma et al.* [1992]
N	37.8	112.3	50.0	351.0	6.0	*Embleton et al.* [1996]
N	38.6	112.0	52.1	354.6	7.0	*Fang et al.* [1988]
N	36.0	110.0	50.9	354.1	7.7	*Zheng* [1992]
N	36.2	110.8	64.8	356.3	3.0	*Tan et al.* [1991]
N[c]	35.0	109.0	42.3	13.7	8.0	*Cheng et al.* [1988]
N	35.5	110.2	67.7	348.9	4.0	*Wu* [1988]
Mean Early Triassic	*N*=7		57.9	352.6	5.4	this study
Upper Permian						
N	35.5	110.3	49.5	358.9	4.0	*Ma et al.* [1992]
N	39.0	111.0	48.6	357.0	7.0	*Ma et al.* [1992]
N	36.0	112.0	56.1	350.3	12.3	*Zheng* [1992]
N	37.5	114.4	55.2	1.4	6.3	*Zhao and Coe* [1989]
N	38.6	112.1	37.9	2.9	6.9	*Zhao and Coe* [1989]
N	40.1	113.2	55.2	335.7	4.7	*Zhao and Coe* [1989]
N	37.8	112.3	47.8	357.4	4.0	Embleton et al. [1996]
N	-	-	44.2	355.9	6.9	*Fang et al.* [1990]
N	42.7	118.9	51.9	341.7	6.8	*Zhao et al.* [1989]
Mean Upper Permian	*N*=9		49.9	354.0	5.3	this study

[a] N, NCB; M, Mongolia; S, SCB; or S-T2-xx, numbers denoting data in Figure 22. [b]poles suspected suffering local rotation. [c] poles lack of detailed demagnetization information or overprinted by secondary magnetization.

SCB and NCB was achieved before the Triassic but that continental shortening continued during the Late Triassic and Early Jurassic. At least 500 km of shortening was suggested in the western part of the Qinling belt. This suggestion is marked by the strong magmatic activity around 220-210 My in the western Qinling and also in the Songpan-Ganze accretion complex. *Reischmann et al.* [1990] also suggested an active continental margin (210 Ma) in the west Qinling. The rotation pole was probably located close to the Dabie area, as shown by the ultrahigh-pressure metamorphism found during the 230-205 My, almost the same age as the paleomagnetically determined rotation [see *Ames et al.*, 1996; *Gilder and Courtillot*, 1997]. The geochronological coherence between the paleomagnetism and the metamorphism favors strongly the suggestion that a final suturation between the two blocks occurred during the Late Triassic.

Poles of Early-Middle Jurassic age from the SCB are statistically similar to that of the Middle Jurassic of NCB, and their error bars intersect with those of the Early Jurassic of the NCB (Figure 21b). Thus both blocks were already sutured (at least within paleomagnetic error bars) during the Middle Jurassic and may be even as early as Early Jurassic. This estimate refines the age of collision and makes it slightly older than the Late Jurassic age estimation of *Gilder and Courtillot* [1997].

Finally, the comparison of our new Chinese APWPs with the one of Europe [*Besse and Courtillot*, 1991; *Van der Voo*, 1993] do not change former conclusions from Permian to Cretaceous times (see the review by *Enkin et al.* [1992b]). The Chinese blocks were remote and not sutured to Siberia before the end of the Jurassic, albeit continental connections were established long time before [*Zhao et al.*, 1990]. On the contrary, recent data of *Ge et al.* [1994] imply a more complex Tertiary history than previously thought. Despite an important dispersion striking on a small circle, the data of *Ge et al.* show that the standstill of China, clearly displayed on our APWP, has most probably persisted during the Paleocene. This situation leads to a Tertiary discrepancy noticed by several authors [*Westphal*, 1993; *Chauvin et al.*, 1996; *Cogné et al.*, 1999] between the Chinese and the "Asian" reference APWP, constructed using transferred data from Atlantic and Indian Ocean bordering continents with the assumption that Siberia is rigidly attached to western Europe. *Cogné et al.* [1999], on the basis of a paleomagnetic analysis of Tertiary poles of central Asia, proposed that this anomaly arises from an inadequate description of the Siberian craton movement, the cause of which could be a non rigid behavior of the Eurasian plate during the Tertiary.

5. Conclusion

Early Triassic and Early-Middle Jurassic poles has been obtained from the southern part of the Sichuan basin. Using Fisherian and small circle iteration techniques, the available Mesozoic data allow us to outline a new Mesozoic APWP for the SCB. The Permo-Triassic data derived from widespread sampling

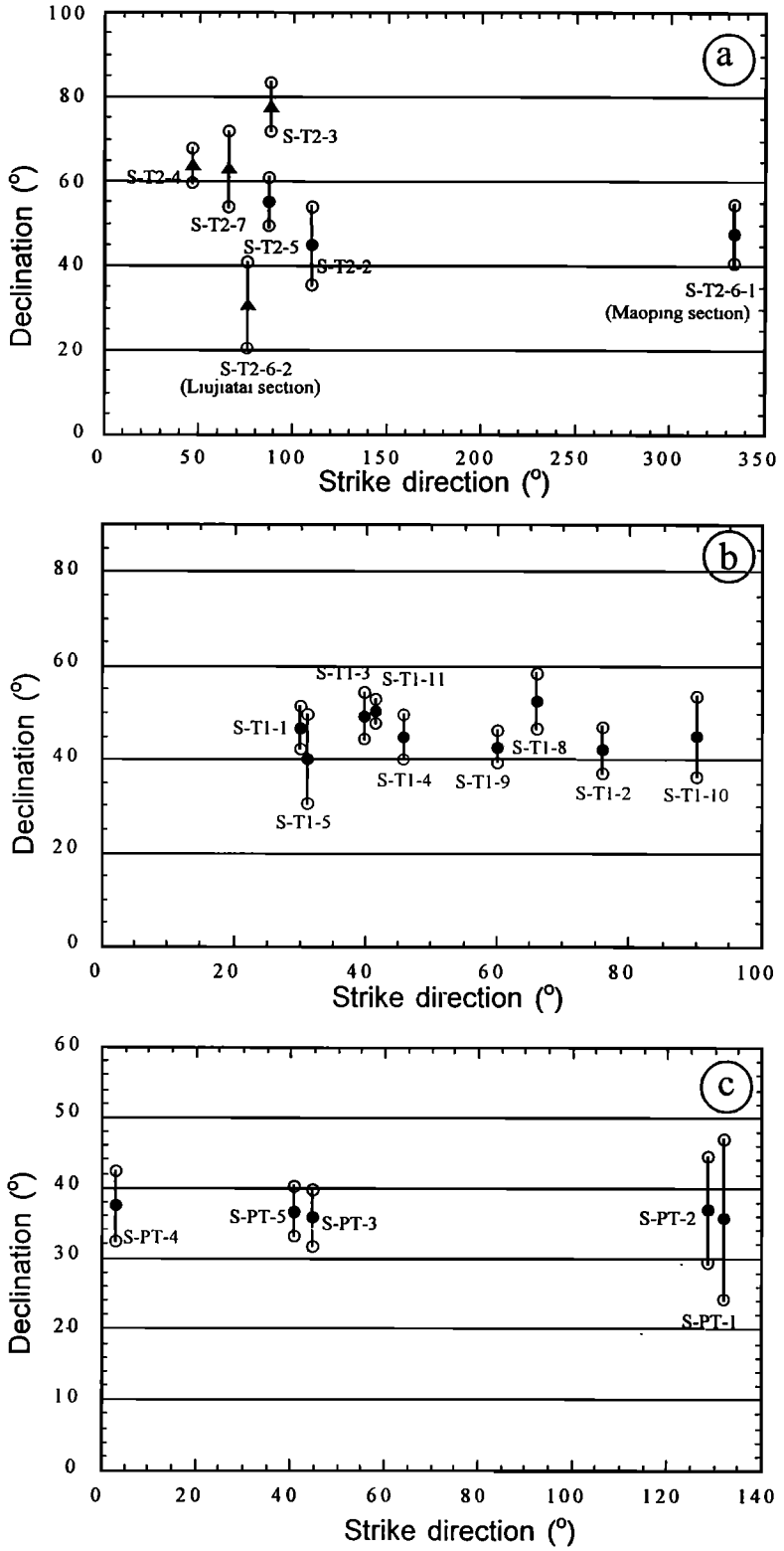

Figure 22. Paleodeclinations with error bars versus fold strike on the SCB for (a) the Middle Triassic, (b) the Early Triassic, and (c) the Permo-Triassic. Numbers next to the data are as in Table 4. Solid triangles indicate that the sampling areas may have suffered local rotations.

areas of the SCB demonstrate no correlation between declinations and the trends of folds, or a major deformation of "oroclinal bending." The small circle dispersion of Late Permian, Permo-Triassic boundary, and Early Triassic poles points to a polar wandering along a tract rather than to the local rotations. A standstill nature of Late Mesozoic poles occurs during the Early-Middle Jurassic, Late Jurassic, and the Cretaceous. From comparision with Mesozoic APWP of the NCB the suturing process between the NCB and SCB was related to the CCW rotation of the NCB and CW rotation of the SCB during the Late

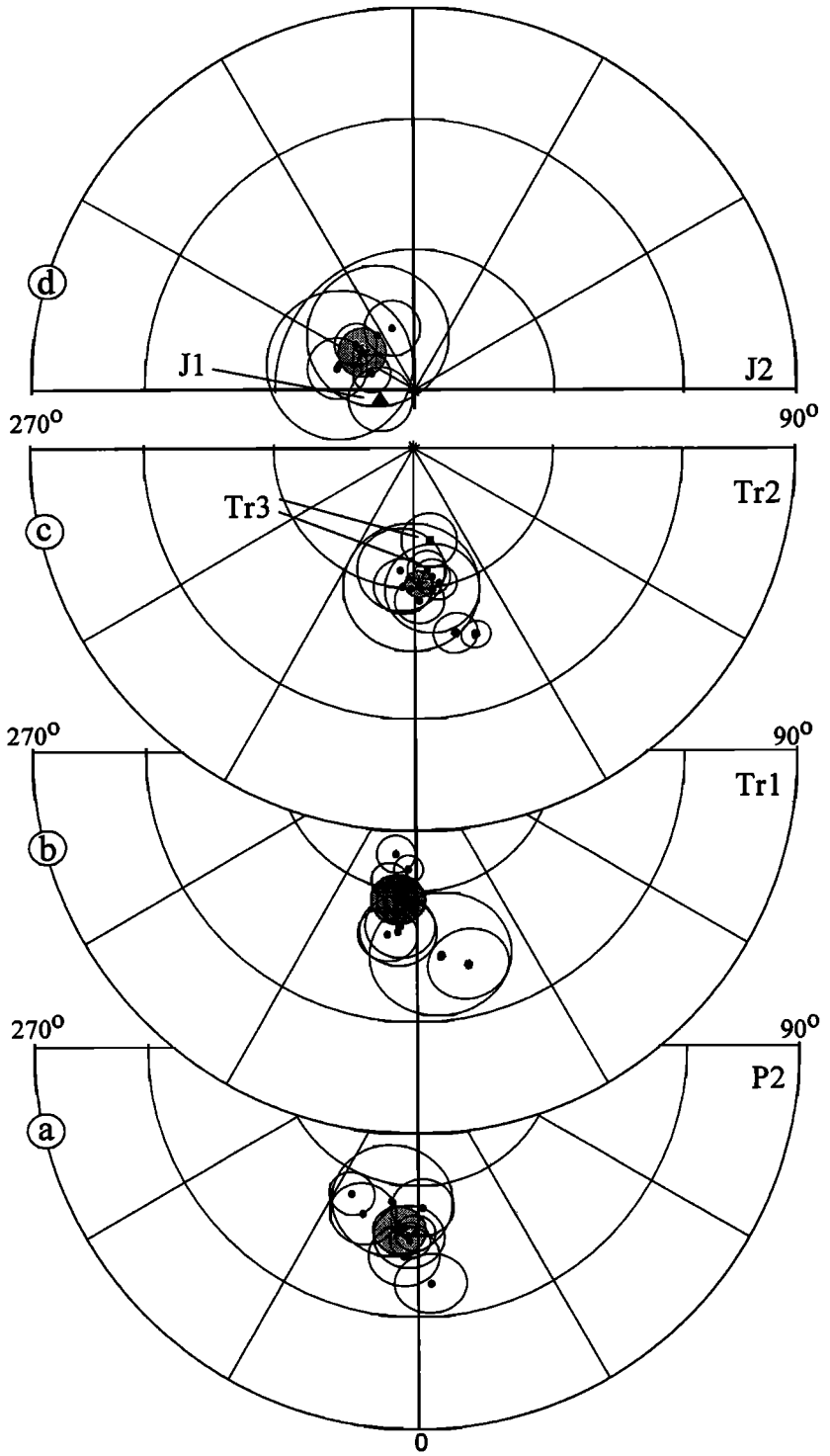

Figure 23. Stereographic north polar projection of paleopoles from the North China Block for (a) the Late Permian (P2), (b) Early Triassic (T1), (c) Middle-(Late) Triassic (T2 and T3), and (d) Early and Middle Jurassic (J1 and J2).

Triassic and Early Jurassic, which resulted in the exhumation of the ultra high-pressure metamorphic rocks in the Dabie and Sulu areas. The overlap of Jurassic poles suggests that final suturing between the NCB and SCB occurred by the Early-Middle Jurassic.

A Late Cretaceous remagnetization related to Late Yanshanian folding in the SCB is revealed in the Triassic and Jurassic sediments, which is consistent with the proposition of widespread Late Mesozoic remagnetization reported in Hubei, Hunan, and Jiangsu provinces [*Kent et al.*, 1987; *Enkin et al.*, 1992a; *Huang and Opdyke*, 1996b, 1997]. The so-called folding-associated remagnetization [*Wang et al.*, 1993], however, is excluded for those rocks.

Acknowledgments. We are very grateful to Baojun Liu for organizing the field trip and to Z. H. Zhuang and X. Z. Jiang for their participation and help in the field and laboratory. This study was supported by the INSU (France) and a NSFC (China) grant 49925410. We wish to thank R. Enkin, F. Heller, and X. Zhao for their careful reviews and comments. We also acknowledge Yo-ichiro Otofuji for providing constructive review of the manuscript. Paleomagnetic data were analyzed using R. Enkin's and J. P. Cogné's computer program packets. IPGP contribution 1715.

References

Ames, L., G. Zhou, and B. Xiong, Geochronology and geochemistry of ultrahigh-pressure metamorphism with implications for collision of the Sino–Korean and Yangtze cratons, central China, *Tectonics, 15*, 472–489, 1996.

Bai, L., H. N. Wu, and R. Zhu, Paleomagnetic result of the Early Triassic from the Wangcang area in north Sichuan, *Sci. China, Ser. D, 27*, 514-520, 1997.

Bai, L., R. Zhu, H. N. Wu, and P. Guo, Paleomagnetism of the Late Jurassic northern Sichuan basin and preliminary study on the true polar wander, *Acta Geophys. Sin, 41*, 324-331, 1998.

Besse, J., and V. Courtillot, Revised and synthetic apparent polar wander paths of the African, Eurasian, North American, and Indian plates, and true polar wander since 200 Ma, *J. Geophys. Res., 96*, 4029-4050, 1991.

Bureau of Geology and Mineral Resources of Sichuan Province (BGMRS), Regional geology of Sichuan Province, report, *Geol. Publ. House*, Beijing, 1991.

Chan, L., Paleomagnetism of Late Mesozoic granitic instrusions in Hong Kong: Implications for Upper Cretaceous reference pole of south China, *J. Geophys. Res., 96*, 327-335, 1991.

Chauvin, A., R. Perroud, and M. L. Bazhenov, Anomalous low Paleomagnetic inclination from Oligocene-lower Miocene red beds of the south-west Tien Shan, central Asia, *Geophys. J. Int., 126*, 303-313, 1996.

Cheng, G., Y. Bai, and X. Sun, Paleomagnetic study on the tectonic evolution of the Ordos Block, north China, *Seismol. Geol., 10*, 81-87, 1988.

Cogné, J.P , N. Halim, Y. Chen, and V. Courtillot, Resolving the problem of shallow magnetization of Tertiary age in Asia: Insights from paleomagetic data from the Qiantang, Kunlun and Qaidam blocks (Tibet, China), and a new hypothesis, *J. Geophys. Res., 104*, 17,715-17,734, 1999.

Courtillot, V., and J. Besse, Mesozoic and Cenozoic evolution of the North and South China Blocks, *Nature, 320*, 86-87, 1986.

Dobson, J. P., and F. Heller, Triassic paleomagnetic results from the Yangtze block, SE China, *Geophys. Res. Lett., 20*, 1391-1394, 1993.

Dobson, J. P., F. Heller, Z. X. Li, and H. Mauritsch, Paleomagnetic and rock magnetic investigations of the Changxing Permo-Triassic boundary sections, Zhejiang Province, China, *Geophys. Res. Lett., 20*, 1667-1670, 1993.

Embleton, J.J., M. W. McElhinny, X. Ma, and Z. Zhang, Permo-Triassic magnetostratigraphy in China: The type section near Taiyuan, Shanxi province, north China, *Geophys. J. Int., 126*, 382-392, 1996.

Enkin, R. J., Formation et déformation de l'Asie depuis la fin de l'ére primaire: les apports de l'étude paléomagnétique des formations secondaires de Chine du Sud, Ph.D. thesis, Univ. de Paris 7, Paris, 1990.

Enkin, R., V. Courtillot, L. Xing, Z. Zhang, Z. Zhuang, and J. Zhang, The stationary Cretaceous paleomagnetic pole of Sichuan (South China Block). *Tectonics, 10*, 547-559, 1991.

Enkin, R. J., V. Courtillot, P. Leloup, Z. Yang, L. Xing, J. Zhang, and Z. Zhuang, The Upper Permian record of Uppermost Permian, Lower Triassic rocks from the South China Block, *Geophys. Res. Lett., 19*, 2147-2150, 1992a.

Enkin, R., Z. Yang, Y. Chen, and V. Courtillot, Paleomagnetic constraints on the geodynamic history of China from Permian to the Present, *J. Geophys. Res., 97*, 13,953-13,989, 1992b.

Fang, D., Y. Guo, Z. Wang, X. Tan, S. Fan, Y. Yuan, X. Tang, and B. Wang, Tectonic implications of Triassic and Jurassic Paleomagnetic results from Ningwu basin, Shanxi Province, *Kexue Tongbao, 2*, 133-135, 1988.

Fang, D., X. Tan, Y. Guo, and G. Yu, Paleomagnetism and tectonic evolution in Mesozoic for north China plate, in *Terrane Analysis of China and the Pacific Rim, Circum-Pac. Counc. for Energy and Miner. Resour., Earth Sci. Ser., vol. 13*, edited by T. J. Wiley, D.G. Howell, and F. Wong, pp. 359-363, Houston, Tex., 1990.

Fisher, R.A., Dispersion on a sphere, *Proc. R. Soc. London, Ser. A, 217*, 295-305, 1953.

Frost, G. M., Paleomagnetic studies on the tectonic evolution of north China and Qaidam, Ph.D. thesis, Univ. of Calif., Santa Cruz, 1994.

Ge, T., G. Liu, L. Fang, S. Zhong, N. Wu, V. Hsu, and A. Baksi, Magnetostratigraphic study of the red beds in the Hengyang basin, *Acta Geol. Sin., 68*, 379-387, 1994.

Gilder, S., and V. Courtillot, Timing of the north-south China collision from new middle to late Mesozoic Plaeomagnetic data from the North China Block, *J. Geophys. Res., 102*, 17,713-17,727, 1997.

Gilder, S., R. S. Coe, H. Wu, G. Kuang, X. X. Zhao, Q. Wu, and X. Tang, Cretaceous and Tertiary paleomagnetic results from southeast China and their tectonic implications, *Earth Planet. Sci. Lett., 117*, 637-652, 1993a.

Gilder, S., X. X. Zhao, R. S. Coe, H. Wu, and G. Kuang, Discordance of Jurassic paleomagnetic data from south China and their tectonic implications, *Earth Planet. Sci. Lett., 119*, 259-269, 1993b.

Gilder, S., R. S. Coe, H. Wu, G. Kuang, X. X. Zhao, and Q. Wu, Triassic paleomagnetic data from Southern China and their bearing on the tectonic evolution of the western-Pacific region, *Earth Planet. Sci. Lett., 131*, 269-287, 1995.

Gilder, S., P.H. Leloup, V. Courtillot, Y. Chen, R. Coe, X. X. Zhao, W. J. Xiao, N. Halim, J. P. Cogné, and R. Zhu, Tectonic evolution of the Tancheng-Lujiang (Tan-Lu) Fault via Middle Triassic to Early Cenozoic paleomagnetic data, *J. Geophys. Res., 104*, 15,365-15,390, 1999.

Heller, F., W. Lowrie, H. Li, and J. Wang, Magnetostratigraphy of the Permo-Triassic boundary section at Shangsi (Guangyuan, Sichuan, China), *Earth Planet. Sci. Lett., 88*, 348-356, 1988.

Heller, F., H. Chen, J. Dobson, and M. Haag, Permian-Triassic magnetostratigraphy-New results from south China, *Phys. Earth Planet. Inter., 89*, 281-295, 1995.

Hsü, K.J., Q. C. Wang, J. L. Li, D. Zhou, and S. Sun, Tectonic evolution of Qinling Mountains, China, *Eclogae. Geol. Helv., 80*, 735-752, 1987.

Hsu, V., Paleomagnetic results from one of the red basin in South China, *EOS Trans AGU*, 68, 295, 1987.

Hu, L., P. Li, and X. Ma, A megnetostratigraphic study of Cretaceous Red Bed from Shanghan, western Fujian, China, Geol. Fujian, 1, 33-42, 1990.

Huang, K., and N. Opdyke, Paleomagnetism of Jurassic rocks from southestern Sichuan and timing of the closure of the Qinling suture, *Tectonophysics, 200*, 299-316, 1991.

Huang, K., and N. Opdyke, Paleomagnetism of Lower Cretaceous to Lower Tertiary rocks from southwestern Sichuan: A revisit, *Earth Planet. Sci. Lett., 112*, 29-40, 1992.

Huang, K., and N. Opdyke, Severe remagnetization revealed from Triassic platform carbonates near Guiyang, southwest China, *Earth Planet. Sci. Lett., 143*, 49-61, 1996a.

Huang, K., and N. Opdyke, Paleomagnetism of Middle Triassic redbeds from Hubei and northwestern Hunan Provinces, south China, *Earth Planet. Sci. Lett., 143*, 63-79, 1996b.

Huang, K., and N. Opdyke, Middle Triassic paleomagnetic results from central Hubei Province, China and their tectonic implications, *Geophys. Res. Lett., 24*, 1571-1574, 1997.

Huang, W., and Z. W. Wu, Evolution of the Qinling Orogeny belt, *Tectonics, 11*, 371-380, 1992.

Kent, D. V., X. S. Zeng, W. Y. Zhang, and N. D. Opdyke, Widespread late Mesozoic to recent remagnetization of Paleozoic and lower Triassic sedimentary rocks from south China, *Tectonophysics, 139*, 133-143, 1987.

Lee, C. Y., On the Szechuan movement, *Geol. Rev., 15*, 135-156, 1950.

Li, H. M., and Z. Wang, Magnetostratigraphy of the Permo-Triassic boundary sections at Changxing, Zhejiang Province, China, *Sci. China, 6*, 652-658, 1989.

Li, Z., I. Metcalfe, and X. F. Wang, Vertical-axis block rotation in southeast China: new paleomagnetic results from Hainan Island, *Geophys. Res. Lett., 22*, 3071-3074, 1995.

Lin, J.-L., M. Fuller, and W. Zhang, The apparent polar wander paths for the North and South China Blocks, *Nature, 313*, 444-449, 1985.

Lowrie, W., Identification of ferromagnetic minerals in a rock by coercivity and unblocking temperature properties, *Geophys. Res. Lett., 17*, 159-162, 1990.

Ma, X., and Z. Zhang, Paleomagnetic study of Permian rocks from Sichuan Emei region and Shanxi Taiyuan region, *Acta Geophys. Sin., 32*, 451-465, 1989.

Ma, X., L. Xing, Z. Yang, S. Xu, and J. Zhang, Paleomagnetic study from the Ordos basin since the Paleozoic, 99 pp., Seismol. Publ. House, Beijing, 1992.

Ma, X., Z. Yang, and L. Xing, The lower Cretaceous reference pole from the north China, and its tectonic implications, *Geophys. J. Int., 115*, 323-331, 1993.

Mattauer, M., P. Matte, J. Malavielle, P. Tapponnier, H. Maluski, Z. Q. Xu, Y. L. Lu, and Y.Q. Tang, Tectonics of the Qinling Belt build-up and evolution of eastern Asia, *Nature, 327*, 496-500, 1985.

Mattauer, M., P. Matte, H. Maluski, Z. Xu, Q. Zhang, and Y. Wang, La limite Chine du Nord-Chine du Sud du Paléozoique au Trias, nouvelles données structurales et radiométriques dans le massif de Dabie-shan (chaine des Qinlings), *C. R. Acad. Sci., Ser. II, 312*, 1227-1233, 1991.

McElhinny, M. W., Statistics of the fold test in paleomagnetism, *Geophys. J. R. Astron. Soc., 8*, 338-340, 1964.

McElhinny, M. W., B. J. Embleton, X. H. Ma, and Z. K. Zhang, Fragmentation of Asia in the Permian, *Nature, 293*, 212-215, 1981.

McFadden, P. L., and M. W. McElhinny, The combined analysis of remagnetization circle and direct observation in palaeomagnetism, *Earth Planet. Sci. Lett., 87*, 161-172, 1988.

McFadden, P.L., and M.W. McElhinny, Classification of the reversals test in palaeomagnetism, *Geophys. J. Int., 103*, 725-729, 1990.

McFadden, P.L., A new fold test for paleomagnetic studies, *Geophys. J. Int., 103*, 163-169, 1990.

Opdyke, N. D., K. Huang, G. Xu, W. Y. Zhang, and D. V. Kent, Paleomagnetic results from the Yangtze Platform, *J. Geophys. Res., 91*, 9553-9568, 1986.

Otofuji, Y., Y. Liu, Yokoyama, M. Tamai, and J. Yin, Tectonic deformation of the southwestern part of the Yangtze craton inferred from paleomagnetism, *Earth Planet. Sci. Lett., 156*, 47-60, 1998.

Pruner, P., Paleomagnetism and paleogeography of Mongolia from the Carboniferous to the Cretaceous, final report, *Phys. Earth Planet. Inter., 70*, 169-177. 1992.

Reischmann, T., U. Altenberger, A. Kröner, G. Zhang, Y. Sun, and Z. Yu, Mechanism and time of deformation and metamorphism of mylonitic orthogneisses from the Shagou Shear Zone, Qinling Belt, China, *Tectonophysics, 185*, 91-109, 1990.

Ren, J., T. Chen, B. Niu, Z. Liu, and F. Liu, *Tectonic Evolution of the Continental Lithosphere and Metallogeny in Eastern China and Adjacent Areas*, 203 pp., Sci. Publ. House, Beijing, 1990.

Steiner, M., J. Ogg, Z. Zhang, and S. Sun, The late Permian/Early Triassic magnetic polarity timescale and plate motions of south China, *J. Geophys. Res., 94*, 7343-7363, 1989.

Tan, X. D., D. Fang, Y. R. Yuan, S. Fang, and J. Bao, Paleomagnetic study on red beds, Liujiagou formation from Taiyuan, Wuqu, Jixian, Shanxi Province, *Acta Geophys. Sin., 34*, 736-743, 1991.

Tan, X. D., C. Liu, and D. Fang, The paleomagnetic study of Triassic rocks from Xinshui basin in Shanxi Province, *Sci. China, Ser. B, 25*, 755-762, 1995.

Tapponnier, P., G. Peltzer, A. Y. Le Dain, R. Armijo, and P. Cobbold, Propagating extrusion tectonics in Asia: New insights from simple experiments with plasticine, *Geology, 10*, 611-616, 1982.

Van der Voo, R., *Paleomagnetism of the Atlantic, Tethys, and Iapetus Oceans*, 441 pp., Cambridge Univ. Press, New York, 1993.

Wang, X., J. G. Liou and H. K. Mao, Coesite-bearing eclogite from the Dabie Mountains in Central China, *Geology, 17*, 1085-1088, 1989.

Wang, Z., and R. Van der Voo, Pervasive remagnetization of Paleozoic rocks acquired at the time of Mesozoic folding in the South China Block, *J. Geophys. Res., 98*, 1729-1741, 1993.

Wang, Z., R. Van der Voo, and Y. Wang, A new Mesozoic apparent polar wander loop for south China: Paleomagnetism of Middle Triassic rocks from Guizhou Province, *Earth Planet. Sci. Lett., 115*, 1-12, 1993.

Webb, L., B.R. Hacker, L. Ratschbacher, M.O. McWilliams and S.W. Dong, Thermal chronologic constraints on deformation and cooling history of high- and ultrahigh-pressure rocks in the Qinling–Dabie orogen, eastern China, *Tectonics, 18*, 621-638, 1999.

Westphal, M., Did a large departure from the geocentric axial dipole hypothesis occur during the Eocene? Evidence from the magnetic polar wander path of Eurasia, *Earth Planet. Sci. Lett., 117*, 15-28, 1993.

Wu, H., Apparent polar wander wander path and paleolatitude distributions for the North and South China Blocks: The geotectonic evolution of the Qinling belt, Ph.D. thesis, Acad. Sin., Beijing, 1988.

Wu, H., L. Zhou, Z. Zhao, Z. Yang and Y. Chen, Paleomagnetic results of the late Paleozoic and Mesozoic from the Alashan area of the northwestern China Block, *Sci. Geol. Sin., 2*, 19-46, 1993.

Yang, Z., and J. Besse, Paleomagnetic study on Permian and Mesozoic sedimentary rocks from north Thailand supports the extrusion model for Indochina, *Earth Planet. Sci. Lett*, 117, 525-552, 1993.

Yang, Z., J. Besse, V. Sutheetorn, J.P. Bassoullet, H. Fontaine, and E. Buffeteau, Jurassic and Cretaceous paleomagnetic data for Indochina: Paleogeographic evolution and deformation history of south eastern Asia, *Earth Planet. Sci. Lett, 136*, 325-341, 1995.

Yang, Z., Y. Cheng, and H. Wang, *The Geology of China*, 303 pp., Oxford Sci., Oxford, England, 1986.

Yang, Z., X. Ma, J. Besse, V. Courtillot, L. Xing, S. Xu, and J. Zhang, Paleomagnetic results from the Triassic sections in the Ordos Basin, north China, *Earth Planet. Sci. Lett., 104*, 258-277, 1991.

Yang, Z., V. Courtillot, J. Besse, X. Ma, L. Xing, S. Xu, and J. Zhang, Jurassic paleomagnetic constraint on the collision of the North and South China Blocks, *Geophys. Res. Lett., 19*, 577-580, 1992.

Yokoyama, M., Y. Liu, Y. Otofuji, and Z.Y. Yang, New late Jurassic paleomagnetic data from the northern Sichuan basin, implication for deformation of the Yangtze Craton, *Geophys. J. Int., 139*, 795-805, 1999.

Zhai, Y., M. K. Seguin, Y. Zhou, J. Dong, and Y. Zheng, New paleomagnetic data from the Hunan Block, China, and Cretaceous tectonics in eastern China, *Phys. Earth Planet. Inter.* 73, 163-188, 1992.

Zhao, X., and R. S. Coe, Paleomagnetic constraints on the collision and rotation of north and south China, *Nature, 327*, 141-144, 1987.

Zhao, X., and R. Coe, Tectonic implication of Permo-Triassic paleomagnetic results from north and south China, in *Deep Structure and Past Kinematics of Accreted Terranes*, Geophys. Monogr., Ser., vol. 5, edited by J.W. Hillhouse, pp. 278-293, AGU, Washington, D. C., 1989.

Zhao, X., R. S. Coe, Y. Zhou, H. Wu, and J. Wang, New paleomagnetic results from northern China collision and suturing with Siberia and Kazakhstan, *Tectonophysics, 181*, 43-81, 1990.

Zhao, Y., The Mesozoic orogenies and tectonic evolution of the Yanshan areas, *Geol. Rev., 36*, 1-13, 1990.

Zheng, Z., Paleomagnetic constraints on the tectonic evolution of the North China Block, Ph. D. thesis, Tokyo Inst. Technol., Tokyo, 1992.

Zheng, Z., M. Kono, H. Tsunakawa, G. Kimura, Q. Wei, X. Zhu, and T. Hao, The apparent polar wander path for the North China Block since the Jurassic, *Geophys. J. Int., 104*, 29-40, 1991.

Zhu, Z. W., T. Hao, and H. Zhao, Paleomagnetic study on the tectonic motion of Pan-Xi block and adjacent area during Yin Zhi-Yanshan period, *Acta Geophys. Sin., 31*, 420-431, 1988.

Zhuang, Z., D. Tian, X. Ma, S. Jian, and S. Xu, Paleomagnetic study of the Cretaceous to Neogene from the Ya'an areas, Sichuan basin, China, Geophys. Geochim. Expl., 12, 224-228, 1988.

J. Besse, Laboratoire de Paléomagnétisme, Institut de Physique du Globe de Paris, 4 Place Jussieu, 75252 Paris cedex 05, France. (besse@ipgp.jussieu.fr)

Z. Yang, Institute of Geomechanics, No.11, Minzu Xueyuan Nan Lu, Beijing 100081, China. (yangzy@public3.bta.net.cn)

(Received December 15, 1999; revised August 28, 2000; accepted September 7, 2000.)